Molecular and Polymer Engineering of Mechanoresponsive Materials for Clinical and Diagnostic Use

Dr. Kenji Tanaka[1]*, Dr. Yuki Sato[1]

[1]Department of Biomedical Engineering, University of Tokyo Hospital, Tokyo, Japan

Keywords: color change, mechanoresponsive, mechanochromic, stimuli-responsive, polymer materials, non-covalent interactions, luminescence

Abstract

The development of mechanophores as building blocks that serve as pre-defined weak linkages has enabled the creation of mechanoresponsive and mechanochromic polymer materials, which are interesting for a range of applications including the study of biological specimens or advanced security features. In typical mechanophores, covalent bonds are broken when polymers that contain these chemical motifs are exposed to mechanical forces, and changes of the optical properties upon bond scission can be harnessed as a signal that enables the detection of applied mechanical stresses and strains. Similar chromic effects upon mechanical deformation of polymers can also be achieved without relying on the scission of covalent bonds. The dissociation of motifs that feature directional non-covalent interactions, the disruption of aggregated molecules, and conformational changes in molecules or polymers constitute an attractive element for the design of mechanoresponsive and mechanochromic materials. In this article we review how such alterations of molecules and polymers can be exploited for the development of mechanochromic materials that signal deformation without breaking covalent bonds. Recent illustrative examples are highlighted that showcase how the use of such mechanoresponsive motifs enables the visual mapping of stresses and damage in a reversible and highly sensitive manner.

1. Introduction

Polymers find widespread application due to the broad spectrum of properties that is attainable, ranging from simple rubbers to high-performance plastics. Many polymer products are exposed to wear and tear in their everyday use and exposure to mechanical force can irreversibly change the material's properties. Beyond macroscopic damages, extensive mechanical forces cause the rupture of individual chains,[1–3] which can ultimately cause failure due to fatigue, creep, or fracture.[4] It is thus crucial to understand how, when, and where such degradation occurs to avoid catastrophic materials failure and to possibly redirect degradation processes into useful responses. Consequently, research efforts directed towards the investigation and development of *mechanoresponsive* materials has drawn ever increasing attention.[2,3,5–8] Polymers that translate mechanical stresses into a defined response are thought to be useful for many different applications, including as tamper-proof packaging materials,[9] as degradable plastics,[10,11] or for structural health monitoring.[12]

One possibility to render polymers mechanoresponsive is the integration of so-called mechanophores. The latter generally feature a weak covalent bond that undergoes either homo- or heterolytic cleavage upon experiencing a force that exceeds a certain threshold.[1,5,7,13,14] These motifs are covalently incorporated into a polymer and serve as pre-defined weak links that preferentially break or transform in response to an applied mechanical force.[1,6,14–16] Widely investigated mechanophores include spiropyrans, 1,2-dioxetanes, and Diels-Alder adducts.[16–18] The rate constants, threshold forces, and transition state bond-lengths and energies of many mechanophores have been well-characterized *via* techniques such as single-molecule force spectroscopy,[19–22] force-modified potential energy surface (PES) modeling,[23] and *in situ* activation using sonication.[2,22,24] The insights gained in such studies have driven advancements in the field of mechanoresponsive materials and the mechanical activation has, for example, been harnessed to promote thermodynamically unfavorable reactions,[19] effect the intra- or intermolecular transfer of protons,[20,25,26] release small molecules,[27] initiate the depolymerization of the surrounding material,[10,28] or elicit changes in the material's color or fluorescence.[16,17,29] The fact that the active bond or functional group of a mechanophore is typically cleaved irreversibly can limit its utility. Some mechanophores can be returned to their original state through an additional stimulus such as light or heat, but unless the mechanophore undergoes a non-scissile cleavage (e.g. a ring-opening reaction, such as in spiropyranes) the reversal is generally hampered by kinetic factors that leave the mechanophore in its cleaved state.[30] An irreversible response can be desirable for some applications,[31] but it also may restrict the functionality of a material or result in a permanent loss of mechanical strength.[5]

An attractive alternative to the use of mechanophores are therefore *non-sacrificial* mechanoresponsive motifs, *i.e.*, chemical motifs, (macro)molecules, or assemblies that respond to mechanical stimuli in a defined manner without undergoing covalent bond scission. In fact, the application of mechanical stimuli can readily elicit conformational changes in individual molecules or polymer chains, disrupt aggregates of molecules, or trigger the disassembly of associated non-covalent binding motifs. In principle, such responses to mechanical forces can always be reversed. For example, directional non-covalent interactions such as hydrogen bonds, π-attractive forces, and metal-ligand interactions generally respond to external stimuli in a reversible manner.[32–36] When employed in polymers, the motifs can not only provide non-sacrificial pathways for the dissipation of energy in response to mechanical deformation, but also endow the host material with a plethora of other properties and functions such as healing capabilities,[33,35–37] enhanced toughness,[38] and improved melt-processing characteristics.[32,39] Furthermore, non-covalent binding motifs can be designed to feature a very wide range of interaction strengths, with association constants (K_a) varying from relatively low values of ca. 10^2 M^{-1} for, *e.g.*, double hydrogen-bonding motifs, up to very high association constants of ca.

10^{14} M^{-1} for the interaction in complexes of tridentate ligands and metal-ions.[32,40] While the strengths of covalent bonds in mechanophores can be varied to some degree by attachment of suitable substituents or the strategic introduction of steric hindrance or ring strain,[41] the achievable range of bond strengths is much narrower than that of mechanoresponsive motifs that do not require the scission of covalent bonds.

What renders non-sacrificial mechanoresponsive motifs useful for monitoring mechanical stresses is their ability to translate an applied mechanical force into a defined signal.[42–48] The most common readout constitutes a change of the color or fluorescence characteristics through interacting small-molecule dye pairs, which in many cases is visually discernible and in all cases spectroscopically detectable. Depending on the type of dye interactions employed, such as excimer formation, fluorescence quenching, or charge-transfer interactions, application of mechanical force can result in a precipitous change of the emission intensity (*i.e.,* an on-off switch). Alternatively, it is possible that the activation (*e.g.,* through dye aggregation or structural changes) causes a shift of the absorbance or emission spectrum, or changes in the fluorescence lifetime.[47,49–51] These characteristics have facilitated the use of such mechanoresponsive motifs in applications as diverse as damage sensing in structural materials[46,52–55] and spatiotemporal analysis of the transmembrane forces in cells.[56] High precision techniques such as atomic force microscopy (AFM), optical tweezers, and electromagnetic tweezers have allowed for a quantitative analysis of non-covalent threshold forces in both biological systems[56,57] and synthetic materials,[58] enabled directly studying the force response on a molecular level,[56,58] and offered insights that allowed tuning the responses to the needs of specific applications.

In the present review article, we aim to give an overview of recent achievements that have been made to develop and use non-sacrificial mechanoresponsive motifs, and hope to provide a perspective towards their future use as versatile moieties that may enable a plethora of new applications in mechanochemistry without relying on the scission of covalent bonds. The first section begins with a discussion of conformational changes in individual small molecules and of interactions between multiple dye molecules to produce visual signals in response to force, including examples such as synthetic capsules that contain aggregachromic dyes, dye-capped telechelic additives, and cross-linking agents that feature dye pairs and act as mechanoresponsive motifs in polymeric materials. The subsequent sections delve into approaches that rely on the use of Förster resonance energy transfer (FRET) processes, charge-transfer interactions, and fluorescent proteins to sense mechanical deformation, before an overview of the use of hydrogen-bonding, host-guest, and metal-ligand interactions as mechanoresponsive motifs with directional non-covalent interactions is provided. Particular emphasis is given to the advantages which these interactions offer for the preparation of materials that display diverse readouts and unique mechanical properties. Finally, we conclude with intrinsically mechanochromic materials that exploit conformational changes in polymers to provide a strain-dependent visual readout. For a detailed discussion of related materials that achieve mechanochromic responses through changes to structural coloration readers are referred to a review article by Clough *et al.* that will appear in *Macromol. Rapid Commun.* as part of this special issue. Instead of discussing the different types of mechanoresponsive motifs in view of their historical development, the sequence in the present review follows from *molecules* to *polymers* and aims to show how individual molecules, molecular aggregates, defined intermolecular interactions, and intra- or intermolecular interactions of macromolecules are harnessed to prepare mechanochromic materials. Throughout the manuscript, selected illustrative examples of the different discussed approaches are thereby highlighted in order to elucidate the underlying principles that can enable the preparation of mechanochromic polymer materials with non-sacrificial mechanoresponsive motifs.

2. Molecular Responses to Mechanical Stimulation

While many of the mechanoresponsive motifs discussed in the present review respond to the application of mechanical forces *via* the cleavage or formation of non-covalent intermolecular interactions, arguably the simplest type of response to mechanical forces is a change in conformation at the molecular level, *e.g.,* stretching or rotation around one or multiple bonds in the same (macro)molecule. Altering the conformation of a (macro)molecule in such a manner can lead to changes of its photophysical properties, which in turn can be harnessed as a signal to detect and potentially measure an externally applied mechanical stimulus,[22] as demonstrated in an early example of mechanochromic polymer materials by Rubner and coworkers with segmented polyurethane-diacetylene copolymers.[59,60] Conformational changes have been employed in both polymer materials and in biological environments to visualize damage or morphological changes that are otherwise difficult to discern.[9,61,62] In the following, the use of mechanoresponsive motifs that rely on conformational changes to develop damage-sensing components for polymer materials is discussed, before their use as force-sensing membrane probes in cells and lipid vesicles is highlighted. Finally, two such mechanoresponsive motifs that undergo conformational changes are presented that are in the early stages of development and which have only recently been investigated in the solid state. Polymeric materials that inherently exhibit a mechanochromic behavior as a result of force-induced conformational changes of macromolecules are presented in Section 5.

2.1. Exploiting Conformational Changes in Molecules

A frequently explored mechanoresponsive motif is that of aggregation-induced emission (AIE) luminogens, for which the chromic response to mechanical force is based on changes to the molecular-level conformational freedom.[63] These molecules only fluoresce when they are confined to certain twisted geometries (*e.g.*, in an aggregated state), whereas the rotational freedom experienced by molecularly dissolved AIE luminogens allows excited states to relax very efficiently through non-radiative pathways. As a result, intramolecular conformational changes in AIE luminogens can lead to striking *on-off* emission changes in response to various stimuli, and such molecules have been incorporated into a wide array of materials to render the resulting materials mechanochromic. After the first AIE luminogen, a pentaphenylsilole, was reported by Ben Zhong Tang and coworkers in 2001,[64] many molecules with a similar structure featuring multiple aromatic groups connected to a core *via* rotationally unrestricted sp^3 bonds were shown to be non-emissive in solution but to luminesce strongly when concentrated or crystallized.[65] This AIE behavior contrasts with the more frequently observed aggregation-caused quenching (ACQ) phenomenon, i.e., the fact that the fluorescence of luminophores that are highly emissive in solution is often quenched in the solid state.[65–67] For example, planar aromatic molecules such as perylene and pyrene derivatives frequently display little to no fluorescence in the solid state, since the formation of aggregates leads to ACQ,[68] and this can limit the utility of such dyes in the context of mechanoresponsive materials design. Strategies to overcome ACQ typically involve the introduction of substituents that frustrate luminophore aggregation.[66,69] However, it was also observed that aggregates of ACQ luminophores could in fact be disrupted by applying mechanical force,[70] which rendered them luminescent. A plethora of studies reported on this type of turn-on fluorescence upon grinding such mechanoluminescent crystalline materials, which has been extensively reviewed elsewhere.[71]

As demonstrated by these grinding examples, the striking turn-on fluorescence of AIE luminogens that can be observed in organic crystals can also be exploited to visualize mechanical deformation. Furthermore, the incorporation of such dyes into other materials can significantly aid in the visualization of mechanical stresses experienced by a host matrix. For example, mechanochromic coatings have emerged as an effective, non-invasive method for identifying damage before failure occurs.[72] Moore and co-workers have exploited the AIE effect of tetraphenylethylene (TPE) (**Figure 1a**), one of the most widely-studied AIE luminogens, to develop mechanochromic polymeric coatings that signal damage with sub-100 µm resolution.[15] The authors encapsulated a hexyl acetate solution of TPE in polyurethane/poly(urea-formaldehyde) core-shell microcapsules, which were then dispersed into a variety of different polymer matrices (*i.e.,* epoxy, polyurethane, PDMS, polystyrene, and polyacrylic acid) and applied as surface coatings to solid substrates.[15] The intact capsules displayed no emission, since the free rotation of the four phenyl groups of TPE leads to non-radiative relaxation of the excited state.[73] When the coatings were scratched or impacted, microcapsule breakage followed by solvent evaporation facilitated TPE aggregation, thus restricting the rotational freedom and causing the damaged areas in the material to brightly fluoresce (**Figure 1b**).[15] Lu *et al.* further explored the damage-sensing capabilities of this approach by incorporating microcapsules containing three different AIE luminogens (TPE, a fumaronitrile, and hexaphenlysilole) with different emission colors at various depths in multilayered epoxy and polyurethane coatings.[74] This allowed for the emission color to be used alongside the fluorescence intensity as a means to obtain high-resolution, three-dimensional profiling of small-scale damage to the polymeric materials.

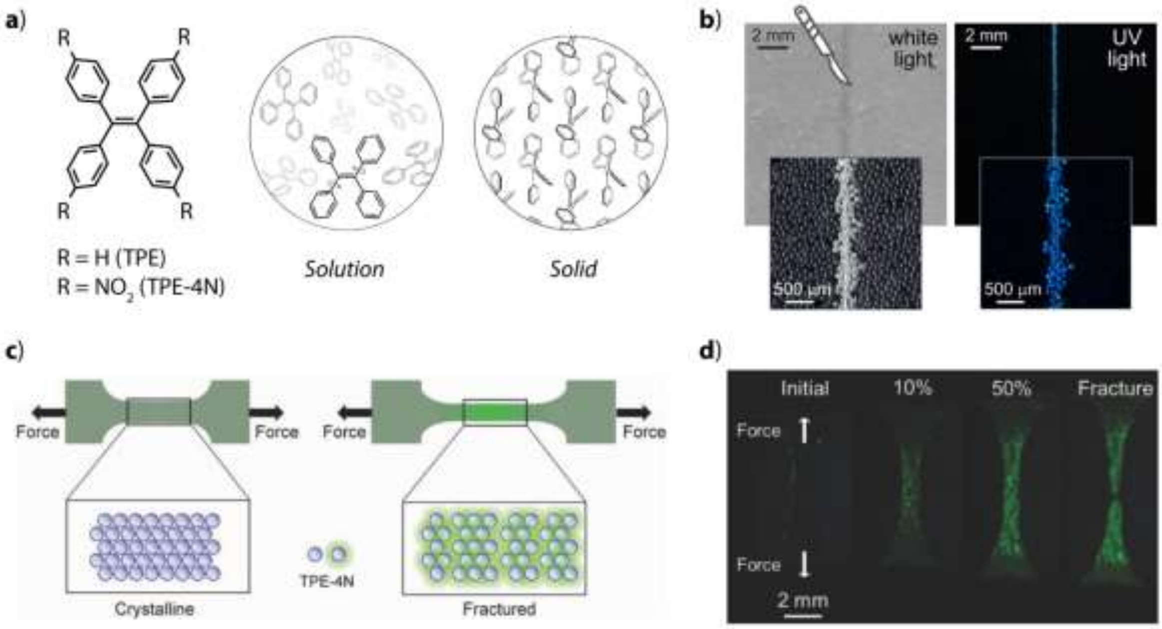

Figure 1. a) Molecular structures of tetraphenylethylene (TPE) derivatives that serve as AIE luminophores and a schematic depiction of the conformational restriction experienced upon aggregation. b) Photographs and microscopy images (insets) of an epoxy coating containing 10 wt % of microcapsules filled with a TPE solution under illumination with white light and UV light after scratching with a razor blade. Reproduced and adapted with permission.[15] Copyright 2016, American Chemical Society. c) Schematic depiction of the turn-on fluorescence response from steel dogbone samples coated with the nitro-substituted derivative of TPE (TPE-4N) depicted in (a). d) Fluorescence images of TPE-4N-coated steel dogbone samples subjected to increasing amounts of strain. Reproduced and adapted with permission.[55] Copyright 2018, John Wiley & Sons.

The utility of AIE luminogens for the preparation of mechanochromic coatings has been further demonstrated with TPE-4N, a derivative of TPE with nitro substituents (**Figure 1a**). TPE-4N fluoresces in its amorphous solid state, but the emission is turned off when samples are crystallized from solution or by annealing amorphous samples at 150 °C. In this case, the nitro substituents quench the emission in crystals by promoting intersystem crossing, a process that is much less efficient in the amorphous state.[75] To exploit the concomitant fluorescence change, Zhong Tang and co-workers casted thin films of the neat TPE-4N onto various solid substrates (*i.e.,* quartz glass, aluminum, ceramic, and wood) *via* spin- and brush-coating techniques. Thermal annealing followed by subsequent cooling allowed for the crystallization of TPE-4N, furnishing coatings that displayed little to no emission.[55,75,76] Upon scratching or by applying pressure, the microcrystalline arrangement of the TPE-4N molecules was disrupted, which relieved quenching from extensive TPE-4N aggregates and resulted in a localized bright green fluorescence. Using this approach, mechanically written high-resolution designs and fingerprints were obtained that could be erased and re-written multiple times.[75] The utility of mechanoresponsive TPE-4N coatings was later extended to stainless steel dogbones and notched samples, for which the authors were able to closely monitor strain distribution and even predict crack propagation, using only a CCD camera and basic image analysis (**Figure 1c,d**).[55] With similar techniques, Zhang *et al.* mapped the evolution of stresses in microstructurally complex steel welding joints while subjecting them to cyclic tensile load.[76] A detailed analysis of the fluorescence response upon mechanical deformation of these TPE-4N coated specimen showed that strains lower than 2% could be reliably detected. These responses of steel substrates with coatings of AIE luminogens provide a simple approach to structural health monitoring, which continues to be of increasing relevance.[12]

The translation of molecular-level conformational changes into easily detectable fluorescence signals has also been exploited to study biological systems, *e.g.*, to analyze the forces experienced in cellular membranes.[61,77] Some of the earliest examples of mechanoresponsive motifs that were employed in membranes comprised a series of hemicyanine-containing oligothiophene molecules developed by Loew and co-workers.[78] These derivatives were found to change both their absorption and emission properties depending on the rigidity and composition of the lipid membrane vesicles into which they were embedded. More recently, Matile and co-workers employed emissive molecules based on an oligothiophene core and substituents that serve as electron donors and acceptors, respectively, as mechanosensitive membrane probes (**Figure 2a**).[42,79] The latter feature a single central bond around which the two rigid components of the molecule can rotate. When free rotation is possible in solution or in a low viscosity environment such as a lipid membrane in its fluid-like state, the two rigid halves of the probe become electronically isolated, and weak, short-lived fluorescence is observed. However, confinement to a planar state by a membrane under tension extends the effective conjugation length of the probe, producing a stronger, red-shifted fluorescence as a clearly discernable signal.[80] It has been demonstrated that such molecular probes can be further customized with various head groups to enable organelle-specific targeting, and their use has provided a reliable way to image membrane tension in cells using techniques such as fluorescence lifetime imagining microscopy (FLIM).[42]

Building on the design of these flipper-type motifs, a new type of papillon (butterfly) probe was recently reported by Matile and coworkers that adopts a bent conformation when exposed to mechanical stresses (**Figure 2b**).[81] The transition between the bent and planar states is accomplished by the swiveling of four *N*-phenyl bonds around two amine fulcra. The conformation change to the bent state is accompanied by a pronounced shift of the emission maximum from 467 to 587 nm. The authors showed that the switching between the bent and planar states can be effected when the probe resides in unilamellar lipid vesicle membranes.[82] When the membrane is compressed from a relaxed and flexible (liquid-disordered, L_d) into a constrained (solid-ordered, S_o) state, the probe is bent, which results in a blue-shift of the emission and enables a spectroscopic analysis of mechanical stress in such vesicles. Thus, two-photon excitation fluorescence (TPEF) microscopy was used to map the distribution of constrained and flexible segments in a multi-component vesicle membrane using the tension-dependent signal from the papillon probe.[82] Moreover, various derivatives with push-pull substituents were prepared.[81] The substitution thereby influenced the energy required to switch from the relaxed to the bent conformer, which in turn enabled the sensing of changes in tension in different types of membranes. In another approach, Sprakel and coworkers recently reported the use of a phenyl-substituted boron-dipyrromethene (BODIPY) derivative as a highly sensitive probe for mechanobiological processes.[83] The viscosity of the surrounding matrix was found to influence the rotational motion of the phenyl substituent, which resulted in a quantifiable change of the fluorescence lifetime. BODIPY derivatives based on this design that allow for targeted binding to the vacuole, cytoplasm, plasma membrane, or cell wall of plants (*Arabidopsis thaliana*) were prepared, and enabled detecting differences in viscosity. For example, a derivative with permanent cationic charges was found to locate in the plasma membrane of a growing root hair, and a lower fluorescence lifetime at the growing tip of the hair than in the epidermal cell membranes indicated an increased membrane tension in areas of ongoing cell division.[83]

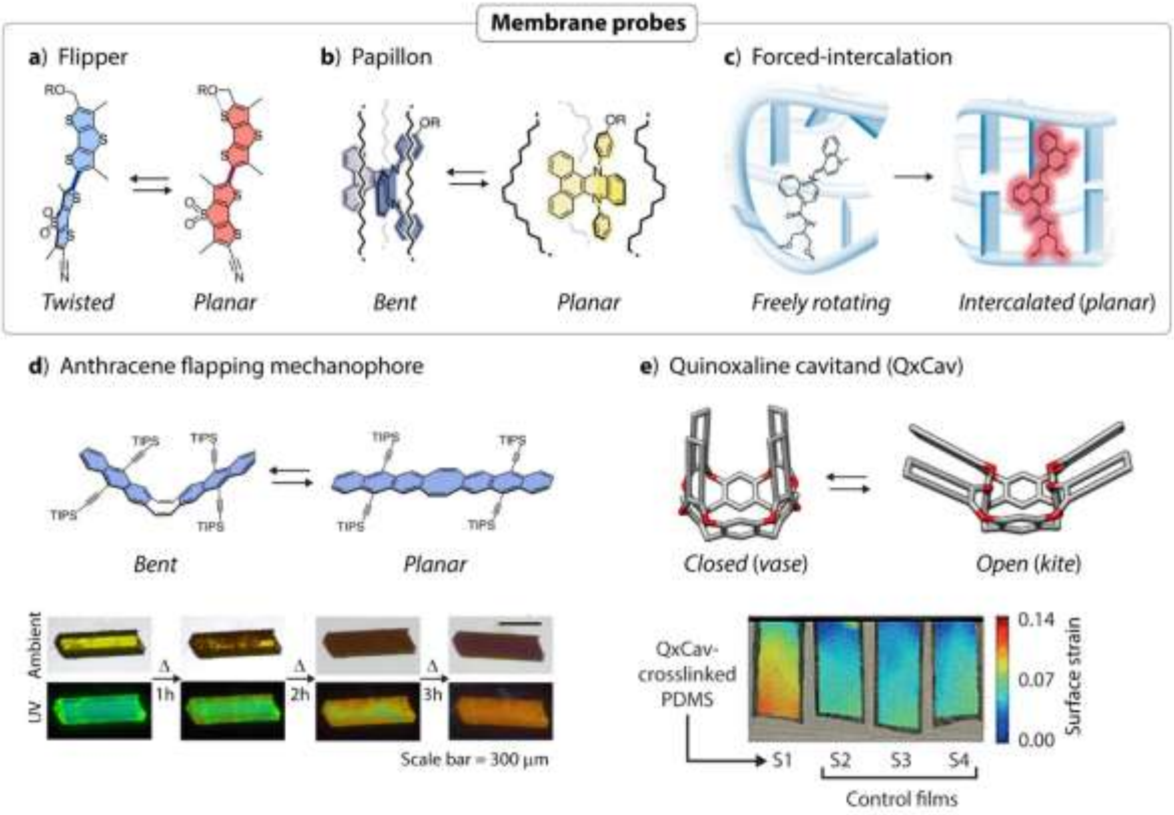

Figure 2. a-c) Molecular structure and conformational switching behavior of different types of membrane probes. Reproduced and adapted with permission.[42,81,84] Copyright (a,c) 2016, 2019, American Chemical Society, (b) 2020, Taylor & Francis. d) Scheme showing the anthracene flapping motif and its conformational switching behavior (top) and images of the changing (fluorescence) color of the crystals when annealed for 3 h at 180 °C (bottom). As the molecule adopts a planar conformation, a gradual color change of the crystals from yellow to brown is observed, concomitant with a change in the dominant emission color from green to orange. Reproduced and adapted with permission.[85] Copyright 2019, American Chemical Society. e) Model showing the opening and closing of the quinoxaline cavitand (top) and images showing the mapping of surface strains of poly(dimethylsiloxane) (PDMS) films cross-linked with the quinoxaline cavitand (bottom). The cavitand was covalently bound to the matrix at the upper rim to facilitate mechanically-induced opening (S1) upon swelling the film. Control samples featuring the cavitand attached only at the bottom (S2), a physical blend (S3), and a neat PDMS film (S4) all show a much lower response. Reproduced and adapted with permission.[86,87] Creative Commons CC BY-NC-ND license 2020, Wiley-VCH and 2018, Georg Thieme Verlag KG.

Mechanoresponsive motifs that rely on conformational changes to elicit a colorimetric response have also found use as so-called forced intercalation (FIT) probes to signal DNA and RNA binding as well as DNA hybridization events with very high specificity.[84,88] To this end, one of the nucleobases of the DNA or RNA sequence can be substituted with a dye and the association to a complementary nucleotide sequence then forces the dye into a confined environment (**Figure 2c**).[89–91] Examples of motifs that have been used in this context include thiazole-, quinolone-,[89] or oxazolopyridine-based[90] dyes with π-conjugated aromatic moieties that are connected by a central double bond. Restricting the rotation around the dye's central double bond leads to an effective planarization of the dye and a turn-on of the fluorescence. When such dyes are integrated into the nucleic acid sequence, successful base-pair binding is translated into a fluorescence signal, which can facilitate high-resolution imaging of RNA hybridization events in both cells and tissue.[89,90] Moreover, Ebrahimi *et al.* employed FIT motifs to signal DNA-analyte binding events using short, single-stranded DNA sequences known as aptamers. Their FIT-aptamer system allows to differentiate Hg^{2+} ions from 14 other metal ions in a buffer solution at concentrations below the toxicity limit, as well as thrombin, a marker of blot clot formation, at concentrations as low as 6.8 nM.[84] At the same time, the generation of any significant false-positive signals in these complex environments was avoided, rendering this a very effective method.

Fluorescence changes in response to the forced planarization of a conjugated molecule have also been realized by Yamakodo *et al.*, who reported the use of a dianthracene derivative as a "flapping" structure (**Figure 2d**).[85] Two anthracene moieties were bridged by a cyclooctatetraene (COT) ring and the molecule preferably adopts a bent conformation with respect to the COT plane. In solution, this bent geometry can easily invert due to the low energy barrier for the interconversion, thus giving rise to a "flapping" motion and an intense anthracene emission. In the crystalline state, the molecules retain the bent configuration but are unable to interconvert, and a bright emission of anthracene excimers is observed. Interestingly, a red-shift in the crystals' fluorescence color from green to orange was seen when the crystalline samples were thermally annealed at 180 °C for 3 hours (**Figure 2d**).[85] The fluorescence change was attributed to a collapse of the molecule into a nearly planar conformation. This was supported by single-crystal XRD analysis, which revealed the dihedral angle of the molecules in the annealed conformation to be between 13–17° compared to 42–49° in the non-annealed state. Only the orange emission was discernible from annealed crystals, suggesting either a complete transformation or very efficient energy transfer.[85] Ultimately, such a behavior could be exploited to give valuable insights into local compressive strains or structural anomalies in a wide range of materials.

The various studies mentioned above speak to the versatility and wide applicability of small molecules as mechanoresponsive motifs in which mechanical forces lead to conformational changes. However, only few studies have so far reported the incorporation of such motifs into polymeric materials. One noteworthy example is the use of a tetraquinoxaline cavitand in poly(dimethylsiloxane) (PDMS)[87] and polyurethane.[86] The cavitand employed consisted of a resorcinarene-based macrocycle with four 2,3-dichloroquinoxaline bridges, which in the closed state, form a deep, “vase”-type cavity with one entry and exit point (**Figure 2e**). In response to a decrease in pH or temperature, upon coordination to Zn^{2+} ions, or exposure to either reducing or oxidizing agents, the 1,4-diazanaphthalene moieties surrounding the cavity switch to an equatorial orientation.[86] The conformational change flattens the structure of the tetraquinoxaline cavitand and drastically increases the exposed surface area,[92] which has been exploited in sensors for volatile organic compounds[93] and for catalysis.[94] Moreover, Torelli *et al.* recently employed the same cavitand as cross-linking agent in PDMS, and reported that conformational switching is observed when films of such samples were exposed to TFA vapors.[87] The cavitand was bound covalently to the polymer matrix at the upper rim of the “vase”, and the accompanying local volume expansion induced by the “vase-to-kite” conformational change caused an increase in the surface strain of these PDMS films of 3% over 60 min of TFA vapor exposure. Using digital image correlation techniques allowed constructing a detailed color map that shows the increase in local strain (**Figure 2e**), and maps obtained upon exposure of control samples that in which the cavitand was either blended into the matrix or covalently attached to the bottom of the "vase" did not display a similar response.[87] In a related study, the authors reported that mechanical stresses applied to polyurethane films that had been cross-linked with a quinoxaline cavitand functionalized with four alcohol groups also stimulated a "vase-to-kite" transition.[86] The conformational change was evidenced by a shift of the UV-Vis spectrum to the absorption band corresponding to the "kite" form at 348 nm (vs. 318 nm for the "vase" form) upon stretching samples to at least 200% strain. Further, the fluorescence spectra showed a shoulder close to 425 nm, which is indicative of the "kite" form (380 nm for the "vase" form), upon applying a strain of 600%. Importantly, these spectral shifts were not observed for cavitands that were only blended into the PU matrix.[86] With these advancements in understanding how the quinoxaline cavitand responds to mechanical force in the solid state, future work could take advantage of the cavity's molecular recognition capabilities to design mechanically recyclable chemical sensors. Furthermore, coupling with suitable small-molecule guest could lead to pH-, temperature-, or redox-switchable mechanical cross-links to afford new types of highly dynamic, tunable materials.

In summary, conformational changes in individual molecules have been successfully exploited as force sensors in a wide variety of bulk materials and biological environments. The fact that these motifs respond to force entirely through non-sacrificial intramolecular transformations in many ways simplifies their implementation, given that they avoid potential complications associated with dynamic equilibria or aggregation processes. A precise understanding of the molecular-level conformational changes that give rise to quantifiable fluorescence signals in these mechanoresponsive motifs has opened up new avenues for the development of highly responsive mechanochromic materials, and, we expect, will continue to enhance the understanding of complex physical processes that characterize the response of different materials to mechanical deformation.

2.2. Responses of Aggregachromic Dyes

Dyes whose emission depends on their state of aggregation are referred to as "aggregachromic"[51] and have been widely used as additives in the fabrication of mechanochromic polymer materials.[95,96] While a variety of photophysical processes can contribute to changes in the emission color, many aggregated aromatic dyes tend to emit as excimers; pyrene, naphthalene, anthracene, and perylene derivatives are prominent examples of such dyes.[97] In contrast to exciplexes, which constitute excited complexes between two different donor and acceptor molecules, excimers are excited dimers that are formed by encounters of two identical fluorophores.[97,98] Formally, an excimer is considered to be a transient state of two molecules that are not associated in the ground state; however, this definition was expanded to include fluorophores that are sterically constrained in close proximity to one another (*e.g.*, pyrene in its crystalline form), and the excimers may not (completely) dissociate after relaxation to the ground state.[98] Thus, a *dynamic* excimer is only associated in the excited state, whereas a *static* excimer arises from photoexcitation of a ground state dimer that is held together by (weak) intramolecular interactions.[99] It has been shown that charge-transfer processes play an important role in the formation of both excimers and exciplexes, however the charge-transfer character is typically more pronounced for the latter.[100] Thus, exciplexes are commonly referred to as charge-transfer complexes,[101] and their use for the preparation of mechanochromic materials will be discussed in more detail in Section 3.2.

From the perspective of fabricating mechanochromic materials, the use of donor-acceptor dye pairs allows one to tune the emission characteristics, but precisely arranging two different dyes in a matrix is significantly more complicated than the use of one excimer-forming dye. Indeed, possibly one of the simplest methods for endowing polymeric materials with mechanochromic properties is *via* blending with excimer-forming dyes.[95,96] When incorporated into a polymer matrix either by melt processing or solvent casting, the dyes tend to form phase-separated aggregates that fluoresce at a characteristic wavelength, which is easily distinguishable from the dyes' monomeric emission in solution. If the aggregates in these blend films are sufficiently small, *i.e.,* with a domain size in the nanometer range, deformation of the films disrupts a sufficiently large fraction of aggregates to effect a blue-shift in the dominant emission color. This concept was first demonstrated by Lowe and Weder in 2002, who infused LLDPE films with an excimer-forming oligo(*p*-phenylene vinylene) (OPV) dye and subjected these films to tensile deformation.[102] The disruption of molecular aggregates led to a change in the emission color from orange to green to is readily discernible under UV light illuminations, and mechanochromic materials have in the meantime been prepared by blending similar OPV derivatives in a wide range of commodity polymers, including polyethylene (**Figure 3a**),[103,104] polyurethane,[105] poly(ethylene terephthalate) (PET),[106] poly(vinylidene fluoride) (PVDF),[107] and polyamide.[108] Moreover, perylene (**Figure 3b**),[109] bis(benzoxazolyl) stilbene (BBS) (**Figure 3c**),[110–112] and poly(phenylene ethynylene)s[113] are examples of other aggregachromic dyes that have been employed in the same manner to render poly(1,4-butylene succinate) (PBS)[114] and poly(propylene)[115] mechanochromic. Despite these successes, approaches towards mechanochromic materials that rely on simply blending such dyes into polymer matrices have largely been limited to semi-crystalline polymers. In the latter, high shear forces arise when the crystalline domains of the polymers are disrupted, and these shear forces are typically required to dissociate the dye aggregates and effect a change in the emission color.[9,96,116] Moreover, the presence of polymer crystals was found to increase the nucleation rate of the dye crystals, and thus led to the formation of smaller, more readily dissociated dye aggregates.[104] The nucleation in amorphous polymer matrices was observed to be much slower, promoting the formation of larger aggregates and rendering the blends less responsive.[51,104] A notable exception where amorphous polymers have been rendered mechanochromic by blending was reported by Porfiri and coworkers; samples of a blend of BBS with a polyurethane (Estane 2103-90AE) were displayed reversible mechanochromism upon uniaxial tensile deformation,[111,112] presumably as a result of specific hydrogen-bonding interactions between the dye and the amorphous polymer matrix.

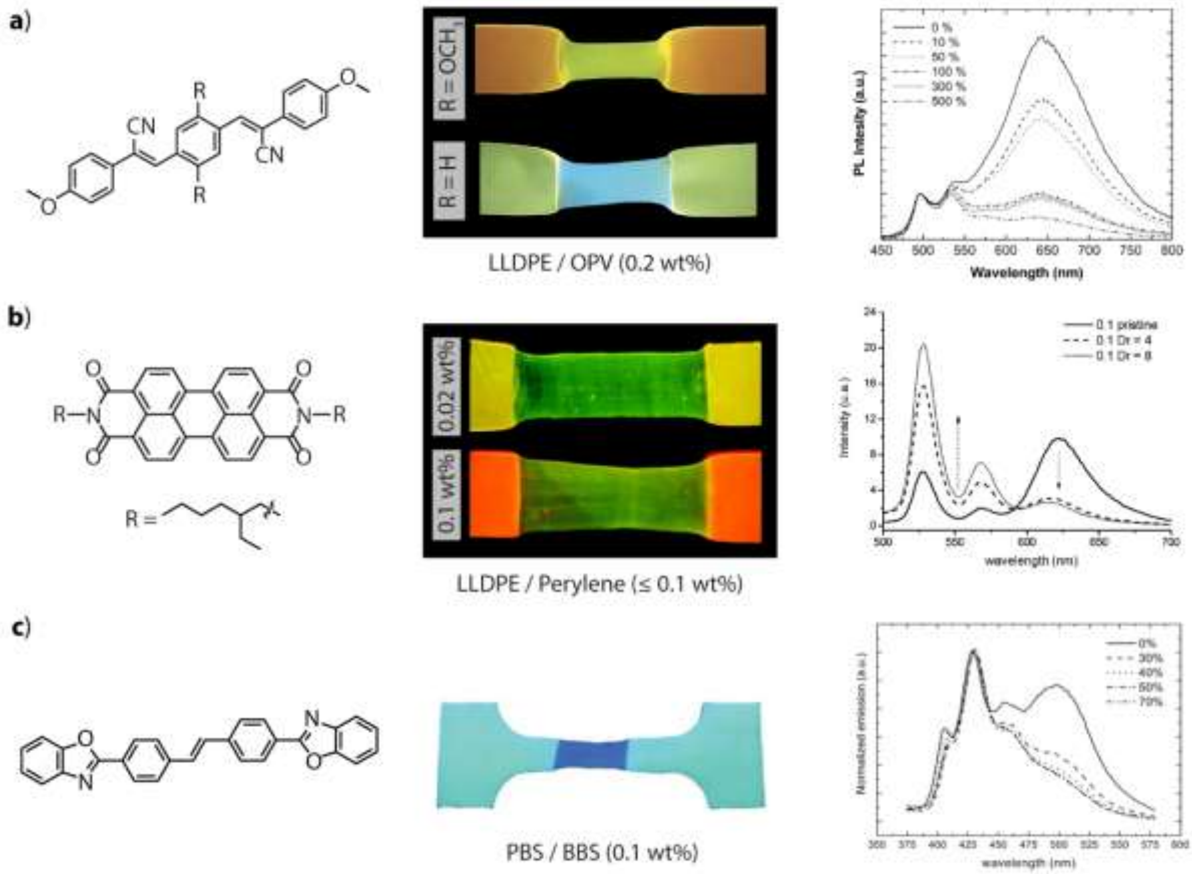

Figure 3. a) Images acquired under UV illumination (365 nm) of films made by blending the depicted cyano-substituted oligo(*p*-phenylene vinylene) (OPV) derivatives with linear low-density poly(ethylene) (LLDPE) and emission spectra for films with OPV (R = OCH_3) showing the mechanochromism upon tensile deformation to 500% strain. Reproduced and adapted with permission.[103] Copyright 2003, American Chemical Society. b) Images acquired under UV illumination (366 nm) of blends of the shown perylene dye with LLDPE after deformation to 300% strain as well as the emission spectra recorded at strains of 0% (bold line), 300% (long dashes), and 700% (short dashes). Reproduced and adapted with permission.[109] Copyright 2008, American Chemical Society. c) Image acquired under UV illumination (366 nm) of a blend of the shown bis(benzoxazolyl)-stilbene in poly(1,4-butylene succinate) after deformation of the sample to 50% strain as well as the recorded emission spectra. Reproduced and adapted with permission.[114] Copyright 2007, Royal Society of Chemistry.

Similar to the studies with AIE dyes (*vide supra*),[15] the encapsulation of aggregachromic dyes and the preparation of polymer composites with these capsules has been recently explored as an effective strategy for producing a mechanochromic response in the absence of significant shear forces. For example, Calvino *et al.* encapsulated a hexyl acetate solution of an OPV dye in poly(urea-formaldehyde) (PUF) microspheres, which were dispersed in an amorphous poly(dimethylsiloxane) (PDMS) matrix to prepare green-fluorescent films.[44] When subjected to externally applied impact, scission, or tensile force, the microcapsules in the films ruptured. After evaporation of the solvent, the OPV molecules aggregated and changed the film's fluorescence color to yellow in the deformed or damaged regions (**Figure 4**).[44] By keeping the internal environment of the intact microcapsules separate from the host matrix, the authors avoided potential dye-polymer solubility issues that can otherwise lead to a suppression of the mechanochromic response. Moreover, capsules that remained intact after mechanical deformation served as an internal standard that allowed to spectroscopically monitor the extent of damage the material sustained. The strategy of encapsulating a color-changing cargo is broadly exploitable,[117] and was further expanded to dyes that display solvatochromism.[118] To this end, a donor-π-acceptor cyanostilbene dye was employed that displays different emission properties in environments of varying polarity, *i.e.*, in different organic solvents versus a polymer matrix. In one example, the cyanostilbene dye was directly blended with various polymer matrices, along with solvent-containing PUF microcapsules; impacting the materials caused the capsules to break, thus solvating the dye near the damaged capsules and locally changing the emission maxima. Conversely, films blended with microcapsules containing the solvated cyanostilbene dye also displayed a change of the emission upon mechanical deformation through impact. In the latter case, however, the change in fluorescence was permanent, whereas the solvent-only capsules furnished a temporary mechanochromic response that lasted only until the released solvent had evaporated.[118]

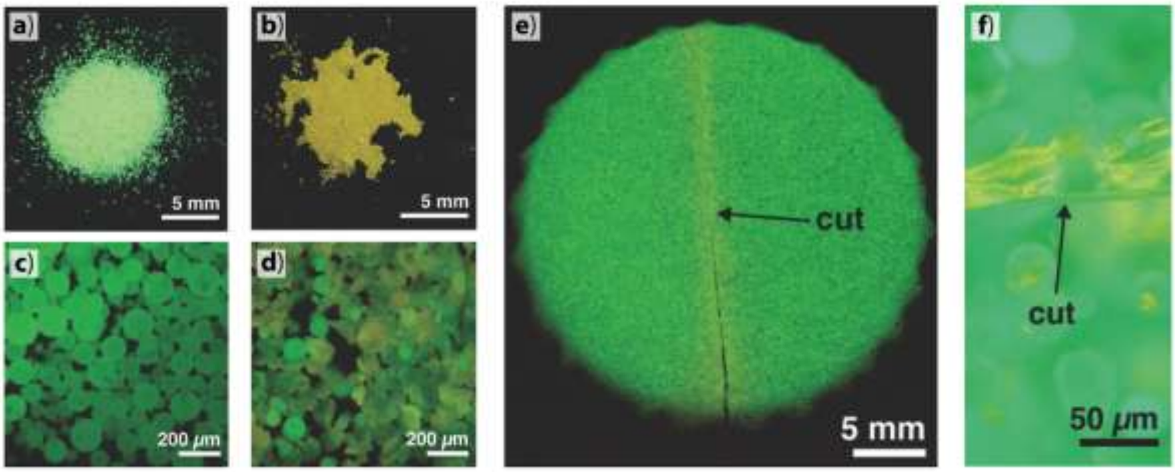

Figure 4. a,b) Photographs and (c,d) micrographs of poly(urea-formaldehyde) microcapsules filled with a hexyl acetate solution of a cyano-OPV derivative before (a,c) and 30 min after (b,d) breaking them. e) Photograph of a PDMS film containing 10 %w/w of microcapsules after incision with a knife showing a color change from green to orange along the cut. f) Fluorescence microscopy image of the damaged area shown in (e). Reproduced and adapted with permission.[44] Copyright 2018, Wiley-VCH.

The aforementioned examples show how the use of microcapsules that carry solutions of suitable dyes can endow virtually any polymeric material with mechanochromic properties, and how the emission color and duration of the response can be tuned. A major disadvantage of this approach, however, is the limited reversibility of the response. To overcome this limitation, Calvino *et al.* developed a telechelic macromolecule that carries an aggregachromic OPV dye at the termini.[119] The macromolecule consists of two OPV molecules covalently attached to the ends of a hydroxyl-functionalized poly(ethylene-*co*-butylene) telechelic polymer (M_n = 3000 g mol^{-1}) and its use as additive in semi-crystalline polymers (*i.e.,* poly(ε-caprolactone) (PCL) and *trans*-1,4-poly(isoprene) (PI)) and an amorphous rubber (*i.e.,* poly(styrene-butadiene-styrene) (SBS)) furnished materials that display an emission color change from orange to green upon tensile deformation and can be followed spectroscopically (**Figure 5**). Importantly, this mechanochromic response, which was monitored spectroscopically by comparing the relative emission intensities of the monomer and excimer states of the OPV dye, was reversible for the highly elastic SBS blend films over at least six cycles. Given that the molecular weight of the macromolecular additive's PEB backbone falls right at the entanglement weight for

PEB,[120] chain entanglement macromolecular additive and the surrounding matrices was suggested as the reason for the improved stress transfer and the robust mechanochromic responses of matrices of differing nature.[119]

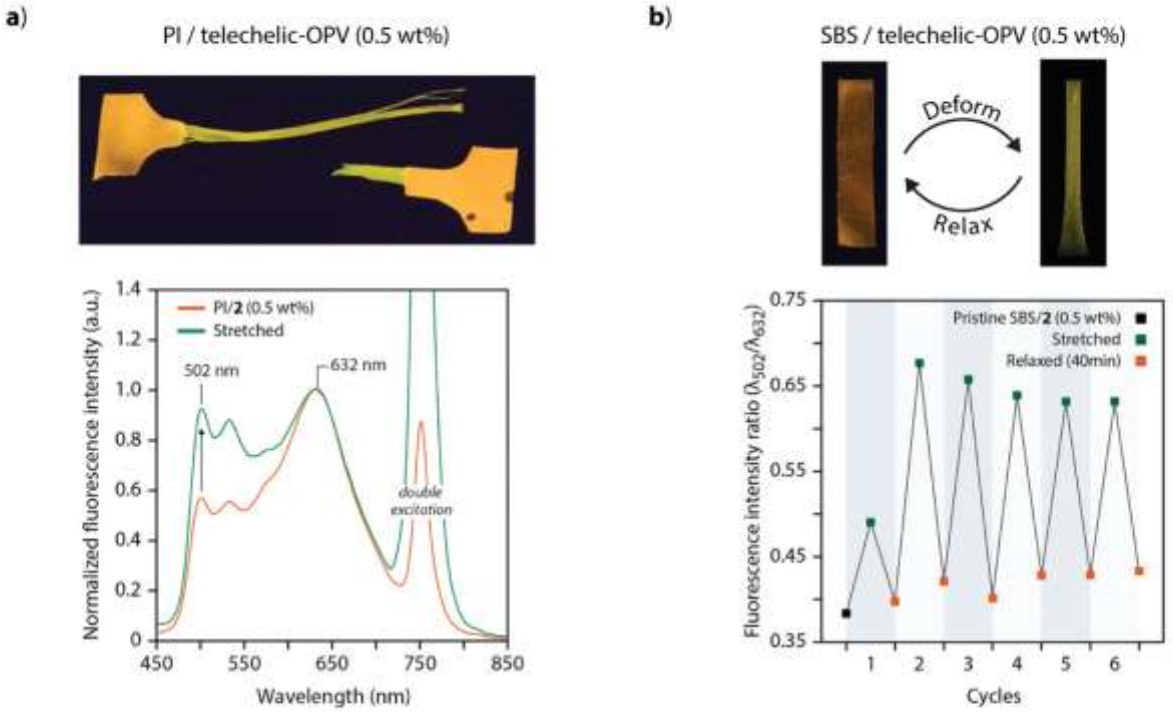

Figure 5. a) Photograph and normalized fluorescence spectra of a thin film of trans-1,4-polyisoprene blended with a macromolecular OPV additive (0.5 wt%) measured before (orange line) and after (green line) tensile deformation until sample failure. b) Photographs showing the reversible fluorescence color change of a poly(styrene-butadiene-styrene) (SBS) film blended with a macromolecular OPV additive (0.5 wt%) upon deformation and a plot of the emission monomer-to-excimer intensity ratio as monitored over six extension-relaxation cycles. All photographs and micrographs were recorded under UV light illumination (365 nm). Reproduced and adapted with permission.[119] Copyright 2018, Wiley-VCH.

To ensure an effective translation of macroscopic mechanical deformation into a mechanochromic response, various strategies have been employed that target the covalent attachment of an excimer-forming fluorophore to a polymer, namely the incorporation of mechanoresponsive motif directly into the backbone of the host polymer,[105] incorporation as part of a loop-type cross-linker,[121] and attachment of aggregachromic dyes as pendant groups.[122,123] For example, Crenshaw *et al.* incorporated an OPV dye into the backbone of a polyurethane; between 4.5 and 9.2 wt% of a dialcohol-terminated OPV was employed as a co-monomer in the melt- or solution-phase polymerization of 1,4-butanediol, poly(tetramethylene glycol), and 4,4-methylenebis(phenyl isocyanate).[105] The elastomers thus produced displayed a significantly more pronounced mechanochromic response upon mechanical deformation than samples of a comparable polyurethane that was blended with an OPV chromophore. While relatively high dye concentration of >4.5 wt% were required to promote aggregation of the OPV moieties and thus create mechanochromic materials, the detailed investigation showed that the covalent attachment of the chromophore prevented the formation of large dye aggregates, which are more difficult to disrupt and effectively enhanced the chromic response.[105]

Covalently attaching two excimer forming dyes *via* a short linker facilitates chromophore aggregation in the as-prepared materials at much lower dye concentrations, as demonstrated by Chen *et al.* for a diacrylate-terminated foldamer structure consisting of two perylene-diimide molecules connected by a short bridge unit.[121] Incorporation of only 0.01 wt% of this foldamer as a cross-linker in a poly(methyl methacrylate) *via* free radical polymerization was sufficient to create compositions that displayed almost exclusively excimer emission. Swelling of the gels with DCM was accompanied by a change of the gels' dominant emission color from bright orange to green, suggesting that the mechanical forces upon expansion of the cross-linked network disrupted nearly all perylene aggregates. Importantly, this process was completely reversed when the gels were dried, and the cycle could be carried out 30 times with negligible loss in the observed fluorescence response.[121] While this work suggests the potential utility of a mechanochromic loop structure in monitoring the forces experienced within a cross-linked polymeric material, further investigation is needed to determine what effect, if any, dilution has on the fluorescence response of the swollen gels, and to what degree the chromophore loops are engaged in intermolecular interactions. These questions will be important in determining to what extent such a motif offers distinct advantages over the covalent incorporation of individual mechanophores.

Despite the aforementioned advantages of covalently incorporating aggregachromic dyes as mechanoresponsive motifs into polymer matrices, the synthesis of such polymers or appropriate loop-type structures can be challenging. As an alternative, Cellini *et al.* reported the preparation of a hydrogel from a poly(*N*-isopropylacrylamide) (pNIPAAm) containing 1 wt% of a pyrene-terminated ethylene glycol methacrylate co-monomer.[122] The polymerization was carried out in the presence of exfoliated Laponite nanoclay to physically cross-link and strengthen the material. The as-prepared hydrogels appeared opaque and light blue under UV light illumination, yet when rectangular films of the hydrogel were subjected to tensile deformation of up to 200% strain, the blue fluorescence of the films became much more pronounced. Furthermore, the increase in blue emission was reversible over at least three cycles of deformation and relaxation, and the shift of the emission bands of pyrene to predominant excimer or monomer emission were directly correlated with the applied uniaxial strain. An approach that uses a polymer with an excimer-forming dye as a pendant group can also be employed to obtain mechanochromic materials from commodity polymers, without the need for solvents or additional reagents. To this end, Zych *et al.* demonstrated that commercial poly(ethylene) (PE) can be rendered mechanochromic by functionalizing maleic anhydride-grafted high- or low-density PE with 1-aminopyrene by simple melt-mixing and extrusion at 160 °C.[123] When tensile force was applied to these materials, the pyrene excimer-to-monomer emission intensity ratio for high-density PE films decreased sharply when necking occurred, while the more extensible low-density PE films showed a gradual increase in the emission intensity ratio up to strains of nearly 1200%.[123]

The changes in the emissive states of such dyes have also been exploited to monitor the formation and dissociation of more complex, higher-order structures that respond to mechanical force. Kato and co-workers were the first to explore the self-assembly behavior of various dendritic pyrene-, anthracene-, and naphthalene-based molecules, showing that these form emissive liquid crystals that change their assembly state in response to both thermal and mechanical stimulation.[124–126,127] A combination of aromatic and H-bonding interactions drive the so-called dumbbell structures to assemble into cubic, columnar, or mesomorphic phases. As a consequence of the extent and geometry of the overlap between the fluorophores at the core of the dendritic structures, each phase displays a different photoluminescence color.[124–126] Moreover, interconversion between the assembled states can be triggered by applying stimuli such as grinding, scratching, or heating/cooling. Building on these results, Sagara *et al.* found that a dendritic pyrene-based molecule, made amphiphilic by the inclusion of hydroxyl functional groups at the dendrite termini, self-assembles in water to form micelles.[128] The hydrophobic fluorophore is shielded from the surrounding aqueous environment, thus leading to yellow excimer emission from the micelle core. Interestingly, grinding the micelles forces the fluorophores to adopt a partially-overlapping orientation, which results in a blue-shift of the emission to a green color.[128] In order to integrate the mechanoresponsive assemblies into polymeric materials, Sagara *et al.* modified the dendritic termini to feature primary amines, which were then used to covalently attach them to microbeads or to the surfaces of living cells.[129] The authors found that vortexing the micelle-coated glass beads shifted the emission color from yellow to green.[129] These findings suggested that the change in emission requires a threshold force, which if determined quantitatively could eventually lead to the use of these dendritic fluorophores as force sensors.

3. Mechanical Stimulation of Hetero-Molecular Complexes

In the approaches discussed in the preceding chapter, mechanochromic responses were realized through changes to either the conformation of individual molecules or by disrupting or forming intermolecular aggregates of the same type of molecule. Whereas the use of a single type of molecule generally facilitates the preparation of a mechanochromic material, the combination of different types of (dye) molecules that form distinct hetero-molecular complexes can be exploited to access materials that display more drastic changes of their photophysical properties in response to mechanical deformation. In the following, mechanoresponsive materials are discussed that feature dye pairs that display an emission due to distinct energy-transfer processes, followed by an overview of materials that exploit intermolecular charge-transfer complexes, and, finally, different examples are examined that rely on fluorescent proteins as the entity that responds to mechanical stimuli through an optical signal.

3.1. Exploiting Förster Resonance Energy Transfer for Mechanoresponsive Materials

In Förster resonance energy transfer (FRET) processes, excited donor molecules transfer energy to an acceptor. Relaxation to the energetic ground state occurs when the acceptor emits a photon. An important requirement for the energy transfer process to occur efficiently is that the emission spectrum of the donor and the absorption spectrum of the acceptor overlap. Besides the spectral overlap and the relative orientation of the transition dipole moments of the dyes, FRET strongly depends on the distance between the donor and acceptor. Thus, the efficiency of the FRET process scales inversely with $(r / R_0)^6$, with r as the intermolecular distance and R_0 as the characteristic distance for which the efficiency of the energy transfer for a donor/acceptor pair is 50%.[101,130] Accordingly, the donor emission is (completely) quenched as long as the donor molecule is in close proximity to the acceptor, while the separation of the donor/acceptor pair results in an increase of the donor fluorescence. Frequently employed FRET donor/acceptor pairs include naphthalene/5-(dimethylamino)naphthalene-sulfonylamide (R_0 = 22 Å)[131] and pyrene/coumarin (R_0 = 39 Å),[132] and their use has been recently reviewed.[133] The high sensitivity of the FRET process to the intermolecular distances renders dye pairs that are capable of energy transfer useful as probes for mechanical transduction processes in- and outside of cells.[101,134] To this end, DNA segments and proteins can be equipped with dyes that display FRET to prepare mechanobiological sensors (molecular tension probes) that allow to observe the relatively small forces that occur in biological systems through an optical readout. For example, Zhao *et al.* developed a membrane probe based on a DNA hairpin structure with a FRET pair to detect and monitor the tensile forces between two cell membranes.[77] Chang *et al.* reported a polymer-based system with a FRET pair that acts as force sensors to detect binding of cells to surfaces,[135] and Wang and coworkers used a short duplex DNA/PNA (peptide nucleic acid) probe conjugated with a FRET pair for similar applications.[136] The interested reader is referred to some excellent reviews that focus the use of molecular tension probes based on FRET in mechanobiology,[134,137,138] while examples that aim to translate the concepts into polymeric materials will be discussed in the following.

Akin to the use of FRET probes to visualize mechanical deformation in aqueous biological systems, hydrogels have been equipped with FRET pairs to access materials that display chromic responses to mechanical stimuli. For example, Walther and coworkers designed a DNA based hydrogel comprising two DNA template strands that were cross-linked by hybridization to short complementary DNA sequences (**Figure 6**). In parallel three different force sensing modules, namely a short DNA double strand (8 base pairs), a long DNA double strand (15 base pairs), and a DNA hair pin structure (8 base pairs), were assembled with complementary DNA fragments that featured a FRET pair of a donor chromophore (Atto$_{565}$) and an acceptor chromophore (Iowa Black RQ).[45] The three different modules featuring the FRET pair and a reference fluorophore (Atto$_{488}$) were incorporated into DNA hydrogels *via* hybridization. In the pristine, relaxed state, the donor and acceptor moieties were in close proximity to each other at the junction of associating DNA base pairs, which acted as cross-links of the hydrogels. Accordingly, only the fluorescence of the reference dye (Atto$_{488}$) was observed. When the hydrogels were placed under tension by uniaxial tensile deformation, however, the relatively short segments of associated DNA strands of the mechanoresponsive modules were dissociated, which was accompanied by a separation of the acceptor and donor moieties and a concomitant increase in Atto_{565} fluorescence (**Figure 6**). While gels with short DNA double strands as cross-links showed an onset of increase in fluorescence from 30% strain, the response of gels with longer DNA double strands only occurred at strains higher than 100%, demonstrating that the mechanochromic response of the system could be readily tailored by adjusting the length of the associating DNA segments. Moreover, replacing the DNA double strand with a DNA hairpin structure that bridges the cross-link rendered the response reversible. When hydrogels with the DNA hairpin cross-links were exposed to mechanical stresses, a fluorescence response similar to the one of gels with long DNA double strands was observed upon uniaxial tensile deformation, but the hairpin served as a permanent linkage that guided the re-association of the DNA segments so that the original fluorescence was recovered after stress relaxation.[45]

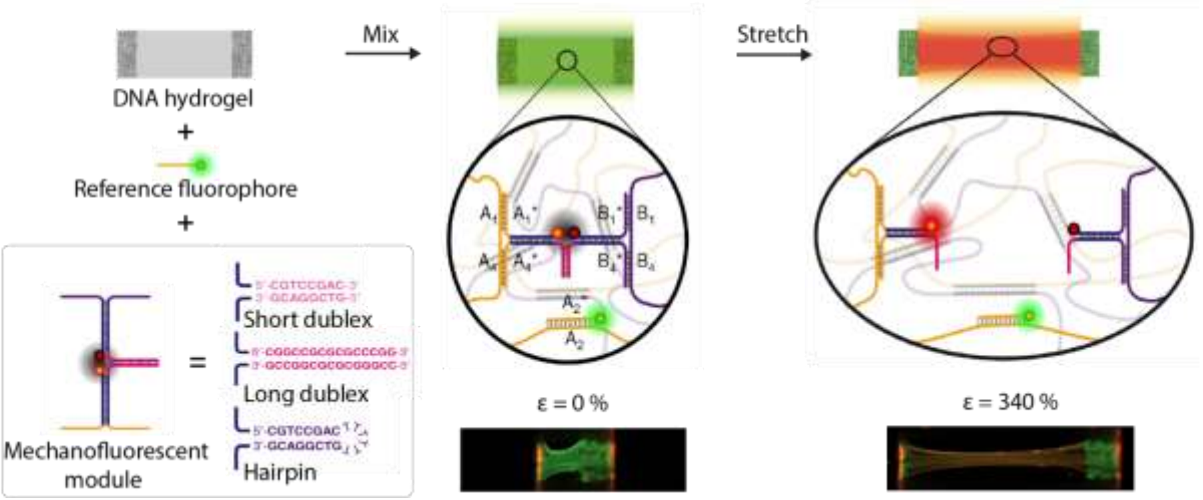

Figure 6. Schematic representation of the self-assembly between a preformed DNA hydrogel with a reference fluorophore (Atto_{488}) and the three different mechano-fluorescent modules into films that display the green fluorescence of Atto_{448}. Stretching of the hydrogel film to 340% strain disassembles the mechano-fluorescent module and orange fluorescence of the previously quenched Förster resonance energy transfer (FRET) donor (Atto_{565}) appears. The process can be imaged as shown in the wide-field fluorescence microscopy images. Reproduced and adapted with permission.[45] Copyright 2019, Springer Nature.

Vogel and coworkers reported how FRET processes can be used in polymer-protein hybrid hydrogels to monitor conformational changes in the glycoprotein fibronectin.[139] To achieve this, fibronectin was modified so that donor (Alexa_{488}) and acceptor (Alexa_{546}) dyes reside in close proximity to each other when the protein adopts its folded, secondary structure (**Figure 7a**). The modified protein featuring the FRET pair was then covalently incorporated into a hydrogel composed of a four-arm star poly(ethylene oxide) (PEG) and poly(*N*-isopropylacrylamide) (pNIPAAm) by a strain-promoted alkyne-azide cycloaddition (SPAAC) reaction. The resulting hydrogel was then immobilized on PDMS as a substrate and the fluorescence response of the composite was monitored upon mechanical deformation. Uniaxial tensile deformation of such samples led to a decrease in FRET intensity, *e.g.*, stretching to 90% strain decreased the median FRET ratio from 0.5 to ca. 0.3 concomitant with an increase in donor fluorescence. Moreover, the response of the samples to mechanical stimulation could be successfully mapped by fluorescence imaging and pixel-by-pixel analysis (**Figure 7b**). Furthermore, Thiele and coworkers reported the preparation of mechanoresponsive micro-gel particles.[140] To achieve this, four-armed, thiol-terminated PEG was labeled with a maleimide-functionalized FRET donor (Alexa_{488}) and acceptor (AlexaFluor_{555}) by thiol-maleimide coupling, and further cross-linking with α,ω-maleimide functionalized linear PEG yielded the desired polymer network. The reaction was carried out in water-in-oil droplets of the precursor solutions that were generated in a microfluidic device to obtain homogenous spherical micro-gel particles with a diameter of 81.5 ± 2.0 μm. Drying of the hydrogel particles resulted in an increase of the FRET efficiency, while swelling of the gel upon exposure to ambient humidity reversed the change and the emission was shifted towards the donor. The particles were compressed by indentation with an AFM tip and a localized increase of the acceptor fluorescence was observed as the donor and acceptor dyes were forced into close proximity (**Figure 7c,d**). The intensity of the particles' response strongly depended on the load applied by the AFM, and forces as small as 1 μN could be calculated to trigger a discernible fluorescence response.[140]

Whereas the aforementioned examples focus on exploiting FRET processes in gels as relatively soft materials, similar donor/acceptor dye pairs have also been used to elicit a mechano-responsive behavior in the solid state in elastomeric materials. For example, Sijbesma and coworkers reported a strain-sensing polymer that relied on the combination of a 7-*N*,*N*-diethylamino-4-methylcoumarin derivative as a donor and a 9-butyl-4-butylamino-1,8-naphthalimide acceptor in a thermoplastic elastomer featuring blocks of soft poly(tetrahydrofuran) and hard bisurea segments.[141] Hydrogen bonding interactions between the urea segments and the methylcoumarin caused the donor to associate with the hard segments, while the acceptor was randomly dispersed in the polymer. Mechanical deformation of samples of such blends to strains of 500% led to a decrease by half of the FRET intensity ratio, which is defined as the acceptor emission intensity divided by the donor emission intensity. However, at small strains the distance between the FRET pairs was not sufficiently altered to furnish a discernible readout based on the FRET intensity ratio. With the aim of improving the response of such systems to mechanical stimulation, the authors explored the use of a telechelic polymer that carried the methylcoumarin donor at the termini and a naphthalimide acceptor in the center. This telechelic was blended with the poly(tetrahydrofuran)-bisurea copolymer, and uniaxial tensile deformation to strains of 100% was found to elicit a decrease in the FRET intensity ratio of ca. 35%.

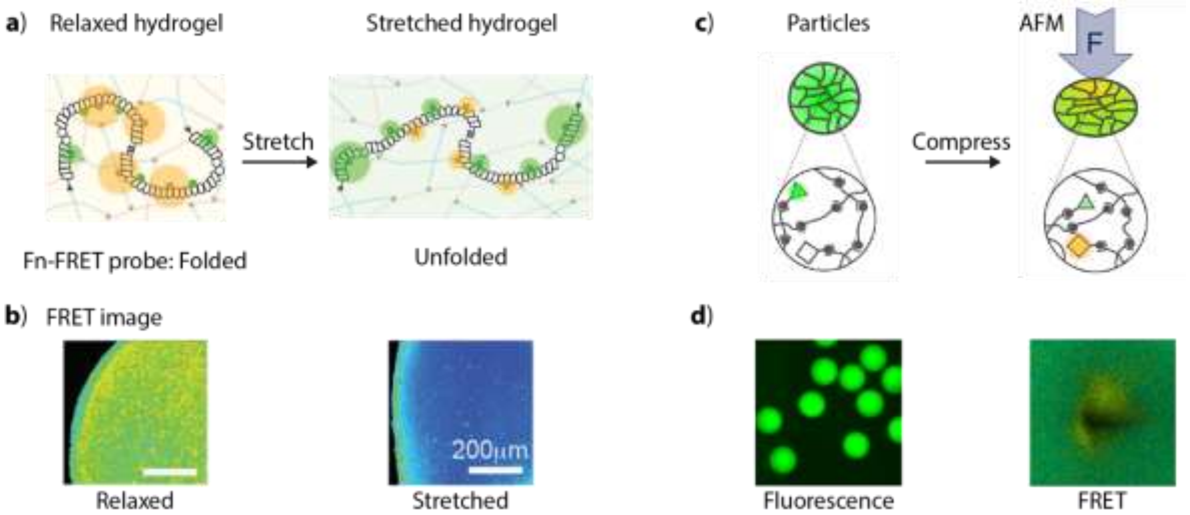

Figure 7. a) Schematic depiction of the fibronectin-based motif bearing Förster resonance energy transfer (FRET) pairs that was embedded in a poly(ethylene oxide) (PEG) and poly(*N*-isopropylacrylamide) hydrogel and responds to tensile deformation by an increase in donor fluorescence. b) Fluorescence microscopy images of the samples described in (a) recorded before and after stretching to 90% strain. Reproduced and adapted with permission.[139] Copyright 2019, Royal Society of Chemistry. c) Schematic depiction of the structure of particles of a DNA-based hydrogel that features a FRET pair to elicit a mechanochromic response. Upon compression of the particles, the dyes of the FRET pair are forced into close proximity, which leads to an increase in acceptor fluorescence. d) Fluorescence microscopy images before deformation as well as imaging during nano-indentation of a hydrogel particle. Reproduced and adapted with permission.[140] Copyright 2019, American Chemical Society.

In a similar approach, Jee *et al.* dispersed rhodamine (donor) and an excess of azulene (acceptor) as a FRET pair in poly(ethylene).[142] Indentation of samples with an AFM tip enhanced the FRET process, as reflected by a decrease of the donor lifetime and an increase of the acceptor emission intensity. These findings are in good agreement with the response observed for gels with FRET pairs that displayed an increased energy transfer efficiency upon compressive deformation. The blending approach was further expanded by Soga and coworkers using PDMS as a matrix.[143] Thus, fluorescein and rhodamine dyes were blended in a ratio of 4 to 1 into PDMS before cross-linking and uniaxial tensile deformation of the dried polymer films to strains of 40% led to an increase in the intensity ratio of the integrated fluorescein and rhodamine emission spectra from 1.3 to 1.5 (**Figure 8a**). Moreover, the same dye pair was also employed to characterize the stress distribution in more complex PDMS samples. Thus, a gradual change in cross-linking density of PDMS samples blended the dye pair was adjusted by the PDMS oligomer/cross-linker ratio. Therefore, a mold was divided into four compartments that were filled with different PDMS oligomer/cross-linker ratio (10:1 to10:4), removal of the barriers, and subsequent curing yielded the gradient film. Image analysis of these samples after mechanical deformation showed that the fluorescein/rhodamine emission intensity ratio is higher (1.8) in more flexible, less cross-linked areas of the sample than in the stiffer regions (1.4).

Takeuchi and coworkers reported that the combination of two bithiophene donors and a porphyrin acceptor into a single, supramolecular "joint" can be employed to elicit a mechanically triggered, FRET-based response that derives from a change of the relative orientation of the transition dipole moments of dyes (**Figure 8b**).[144] Thus, a porphyrin acceptor was employed as the central moiety and bithiophene donor moieties were installed on the opposing faces of the porphyrin in a manner that conformationally constrained the donors to orient out of the plane of the acceptor core. The joint-type moiety was then integrated as a cross-linker into PDMS, and tensile deformation of the films led to a re-orientation of the donor moieties relative to the acceptor so that the transition dipole moments aligned in a manner that furnished an increased FRET efficiency and acceptor emission. The interlocked joint architecture of this mechanoresponsive motif allowed for a recovery of the initial FRET efficiency when the strain was released. This example highlights how FRET-based processes could be employed to create mechanoresponsive systems in a range of different materials, and there appear to be many more opportunities to create systems that enable an in-depth characterization of changes that occur in biological or polymeric materials upon exposure to mechanical stimuli.

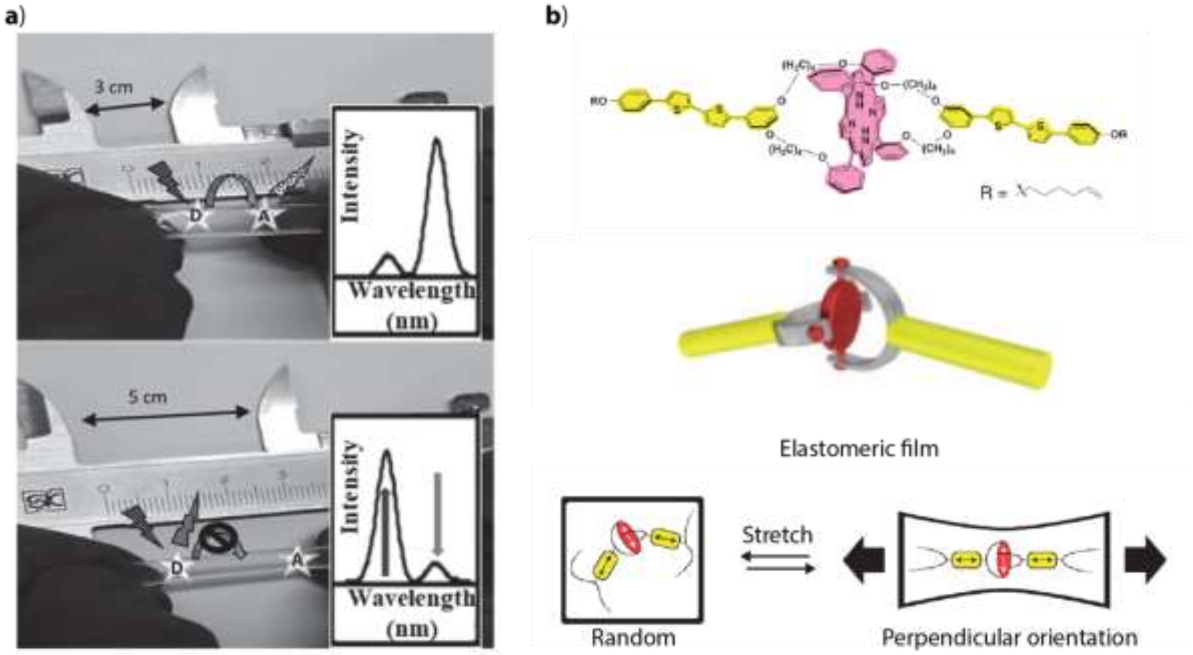

Figure 8. (a) Photographs showing the strain dependent response of a polymer featuring a mechanoresponsive motif that relies on a Förster resonance energy transfer (FRET) process. In the relaxed state, poly(dimethylsiloxane) (PDMS) blended with fluorescein (donor) and rhodamine (acceptor) display acceptor fluorescence due to the close proximity of the dyes, while stretching of the material to 40% resulted in a distinct increase of the donor/acceptor fluorescence ratio. Reproduced and adapted with permission.[143] Copyright 2018, Society of Photopolymer Science and Technology. (b) Schematic depiction of an orientation-based FRET motif. The supramolecular joint structure composed of a phorphorine acceptor and a bithiophene donor was covalently embedded into PDMS and stretching of the film revealed a reversible conformational change from random to perpendicular orientation of the joint, which caused an increased FRET efficiency and acceptor emission. Reproduced and adapted with permission.[144] Copyright 2011, Chemical Society of Japan Society.

3.2. Mechanoresponsive Materials with Charge-Transfer Complexes

Charge-transfer complexes can form through a photo-induced electron transfer process by which an electron-rich donor molecule transfers an electron to the electron-poor acceptor.[101] The charged complex can relax to the energetic ground state by photon emission from the excited complex (exciplex) or by thermal depopulation processes. However, charge-transfer complexes can display a very high stability and do not necessarily relax back to the ground state, as reported for prominent examples such as the complexes between tetracyanoquinodimethane (TCNQ) and tetrathiafulvalene (TTF) derivatives.[145] The complexes typically display a pronounced charge-transfer band in the UV-Vis spectra and the absorption is frequently in the visible range so that a strong coloration is observed. For the preparation of materials that respond to mechanical stimuli both, the formation as well as the dissociation of such charge-transfer complexes between electron donor and acceptor moieties can be exploited, and the varying strength of the complexes can be used to tune the behavior.

For example, the formation and dissociation of the charge-transfer complex between trinitro-fluorene and anthracene was probed in single molecule force spectroscopy (SMFS) experiments.[146,147] For this purpose, trinitrofluorenone was immobilized on an AFM tip while anthracene was grafted on quartz surfaces. The pull-off force of the multiple intermolecular complexes was determined to be ca. 6.6 nN in dodecane (a good solvent for the formation of the CTC complex), while the use of a competitive solvent like 1-methylnaphtalene decreased the force to 1.7 nN,[147] demonstrating how the immediate environment influences the response of such complexes to mechanical stimuli. More recently, the use of charge-transfer complexes was explored for the preparation of microcapsule-based damage reporting polymer materials by Lavrenova *et al*.[148] In this case, a colorless hexamethylbenzene donor and a chloranil acceptor were separately dissolved in toluene and encapsulated in poly(urea-formaldehyde) microcapsules that were prepared in an emulsion polymerization. The prepared microcapsules were then blended into PDMS. Compression, stretching, or indentation of the resulting composites damaged the capsules, which led to a release of the donor and acceptor solutions and the formation of a visually discernible color change on account of the formation of the red charge-transfer complexes.

The use of relatively strong charge-transfer complexes allows for the preparation of materials that display a clear, visually discernible response, but it can be difficult to reverse the association of such complexes. Thus, the dissociation of stable charge-transfer salts is not straightforwardly achieved inside polymer matrices. Significantly weaker interactions between dye pairs that display photo-induced energy transfer can also be employed for the preparation of mechanoresponsive motifs, as recently demonstrated with mechanically interlocked rotaxane structures by Sagara, Weder, and coworkers.[47] In a first embodiment of this approach, rotaxanes were prepared that comprise a macrocycle featuring a π-extended benzothiadiazole donor bearing a cyclophane moiety interlocked with a naphthalene-bisimide-bearing dumbbell as a fluorescence quencher.[47] The rotaxane was then covalently embedded into a polyurethane matrix by copolymerization with poly(tetrahydrofuran), methylene diphenyl diisocyanate, and butane diol. In pristine samples of the rotaxane-containing polymer, the formation of a (weak) complex that displays photo-induced energy transfer drives the donor to be located in close proximity to the quencher. Whereas the fluorescence of the benzothiadiazole donor was completely quenched in the relaxed state, uniaxial tensile deformation of samples led to a separation of the fluorophore and quencher moieties, and a bright green fluorescence was observed. The fluorescence switch-on behavior of the rotaxane-based mechanoresponsive motif was reversible over multiple cycles and temperature-independent. Moreover, the emission intensity was found to increase linearly with the applied strain and the response directly mirrored the stress relaxation behavior of the polymer.[47] Following the same approach, Weder, Sagara, and coworkers developed a series of different rotaxane-based motifs that display different emission colors including blue, green, and orange on account of switching the implemented luminophores while maintaining the structure of the dumbbell (**Figure 9a,b**). Moreover, the preparation of polymers that feature rotaxanes with different emission colors (blue, green and orange) in the appropriate ratio resulted in a material that emits white light in response to tensile deformation.[149] Further exploring their utility, polymers were prepared in which the dye separation in the pristine, rotaxane-bearing polyurethane leads to a trapped state.[150] Thus, a cyclophane-based macrocycle was threaded onto a dumbbell with a boron-dipyrromethene (BODIPY) dye to furnish a red-light emitting rotaxane. Covalently embedding the latter into a PU matrix caused the rotaxane to remain in a trapped state in which the fluorophore and quencher moieties were separated. However, complete quenching of the BODIPY emission was achieved by plasticizing samples with phenylacetonitrile, and a strong and reversible fluorescence response was observed for such plasticized samples upon tensile deformation to 600% strain, even though the material was much softer than dry PU samples.

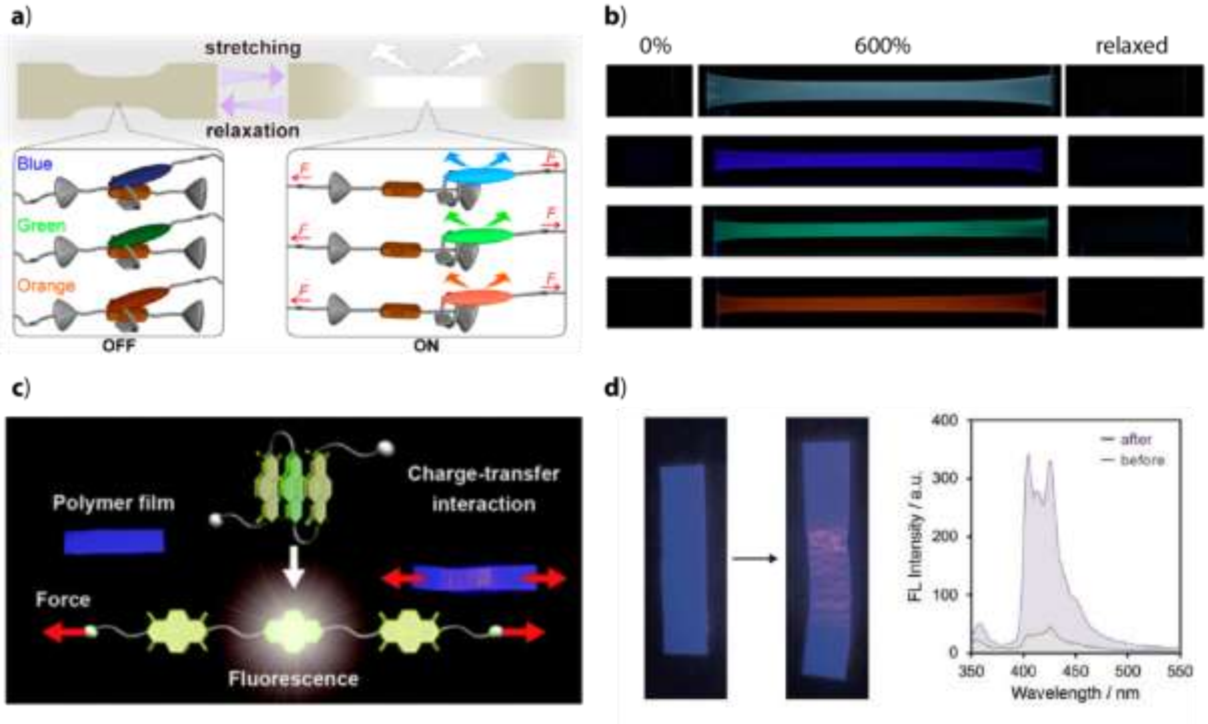

Figure 9. a) Schematic depiction of rotaxanes composed of a macrocycle with a donor dye interlocked with a naphthalene-bisimide-bearing dumbbell as a fluorescence quencher. Altering the luminophore enables the preparation of mechanochromic materials that display blue, green, or orange emission, and samples that are white-light-emitting were successfully prepared by mixing polymers featuring the different emission colors (blue/green/orange emitting polymers in a ratio of 8:16:5). b) Photographs taken under UV light illumination (365 nm) of the polymers with the rotaxanes at 0% strain (left), while stretched to 600% strain (center), and following relaxation to 0% strain (right) show the reversible fluorescence response of the polymers with the rotaxane-based motifs. Reproduced and adapted with permission.[149] Copyright 2019, American Chemical Society. c) Schematic depiction of a mechanoresponsive motif based on the charge-transfer interaction between pyrene and two naphthalene diimide molecules, that were linked to each other by short oligo(ethylene glycol) linkers and covalently embedded into poly(ε-caprolactone) (PCL). d) Photographs of PCL films containing the mechanoresponsive motif before and after stretching under UV light (365 nm) and the corresponding fluorescence spectra of the film, which indicate a fluorescence intensity increase after stretching of the sample. Reproduced and adapted with permission.[151] Copyright 2020, Royal Society of Chemistry.

By exploiting charge-transfer interactions, Takeda and coworkers recently reported a novel mechanoresponsive motif that relies on the non-covalent association between covalently linked pyrene and naphthalene diimide moieties.[151] Two structures were prepared by linking a short oligo(ethylene glycol)-bearing pyrene moiety in either a 1:1 or 1:2 stoichiometry to a naphthalene diimide derivative by means of a CuAAC reaction (**Figure 9c**).[151] A comparison of the solution-phase UV-Vis absorption and fluorescence spectra of the prepared motifs with a 1:1 and 1:2 ratio of the donor and acceptor dye showed that the latter displayed a more intense charge-transfer band and improved quenching of the pyrene fluorescence. Both structures were subsequently covalently incorporated into a PCL matrix by ring-opening polymerization of ε-caprolactone and, similar to the behavior in solution, samples with the dye pair in a 1:2 ratio showed superior fluorescence quenching. The corresponding samples were accordingly chosen for investigations of the mechanoluminescence. After solvent casting, pristine films showed the band corresponding to the charge-transfer complex and the pyrene fluorescence was effectively quenched. Upon mechanical deformation by manual stretching, the fluorescence intensity of the pyrene moieties was observed to increase, indicating the disruption of the charge-transfer complexes (**Figure 9d**). In line with the plastic deformation of the samples, change in fluorescence intensity was irreversible.

3.3. Fluorescent Proteins as Mechanoresponsive Motifs

In addition to integrating FRET pairs into proteins and DNA segments for tension probes in biological systems, the unique features of fluorescent proteins have also been explored for the preparation of mechanochromic materials. In particular, the green fluorescent protein (GFP) and yellow fluorescent protein (YFP) have been used as strain and tension sensors in studies that focused on mechanical processes in biology.[152] Both proteins feature a similar amino acid sequences and fold into secondary structures that result in the formation of a hydrophobic cavity.

The latter bears a *p*-hydroxybenzylidene imidazoline chromophore, which fluoresces green as long as it is stabilized by the protein's secondary structure. YFB features an additional phenol moiety (Try203) in proximity to the chromophore and the overlap between the two moieties results in a shift of the fluorescence emission.[153,154] However, when the distinct secondary structures of GFP or YFB are altered in response to applied stimuli, the bright green or yellow fluorescence is changed. For example, altering the distance between the *p*-hydroxybenzylidene imidazoline chromophore and the phenol moiety in YFP leads to a blue-shift of the emission, and unfolding of the proteins causes a complete loss of the fluorescence. Both, simulations and experimental studies by single molecule force spectroscopy in combination with fluorescence spectroscopy measurements have been used to gain a detailed understanding of the correlation between the secondary structure of the proteins and the fluorescence response.[155] Moreover, mutations of the protein were explored to elicit higher stability,[156] a response to hydrostatic pressure,[157] analysis of interactions during cell adhesion.[158] Many more examples have been reported that target a response to the small forces observed in biological systems.[158,159]

In addition to these applications of the GFP and YFP proteins as force and strain sensors in biological systems, their utility for the detection of forces in bulk polymeric materials has also been explored. For example, Bruns and coworkers used a YFP derivative to analyze the force distribution in fiber-reinforced polymer composites.[53] In this case, enhanced yellow fluorescent protein (eYFP) was covalently immobilized at the interface between glass fibers and an epoxy-based polymer matrix by reacting an *N*-hydroxysuccinimidyl-activated ester at the glass substrate with an amine group of the protein and subsequent application of an epoxy top layer. Mechanical deformation of the composite materials by impact testing was observed to lead to the delamination of the epoxy resin matrix from the glass fibers and resulted in a concomitant quenching of the fluorescence as the proteins at the interface unfolded (**Figure 10a,b**).[53] The principle was also expanded by the same group to composites of a commercial epoxy resin with carbon nanofibers.[52] In these composites, the secondary structure of the eYFP protein hinders the quenching of the fluorescence emission that is otherwise frequently observed when chromophores are placed in close proximity to carbon fibers.[160] This allowed for a visualization of fractured fibers as unfolding of the eYFP and concomitant decrease in its fluorescence occurred when the composite materials were subjected to impact testing.[52] Similarly, Brantley *et al.* prepared blends of eYFP protein and poly(methyl methacrylate) (PMMA) and observed that the compression of such blends with a pressure of up to 360 MPa caused a hypsochromic shift of the emission maximum from 539 to 534 nm **(Figure 10c).**[153] Additionally, GFP was covalently incorporated into PMMA by free radical polymerization of methyl methacrylate in the presence of genetically modified GFP bearing cysteine residues on opposite sides of the protein's barrel-type secondary structure. Compression of the samples with a pressure of up to 41 MPa led to a gradual decrease in fluorescence intensity as the protein unfolded (**Figure 10d**).

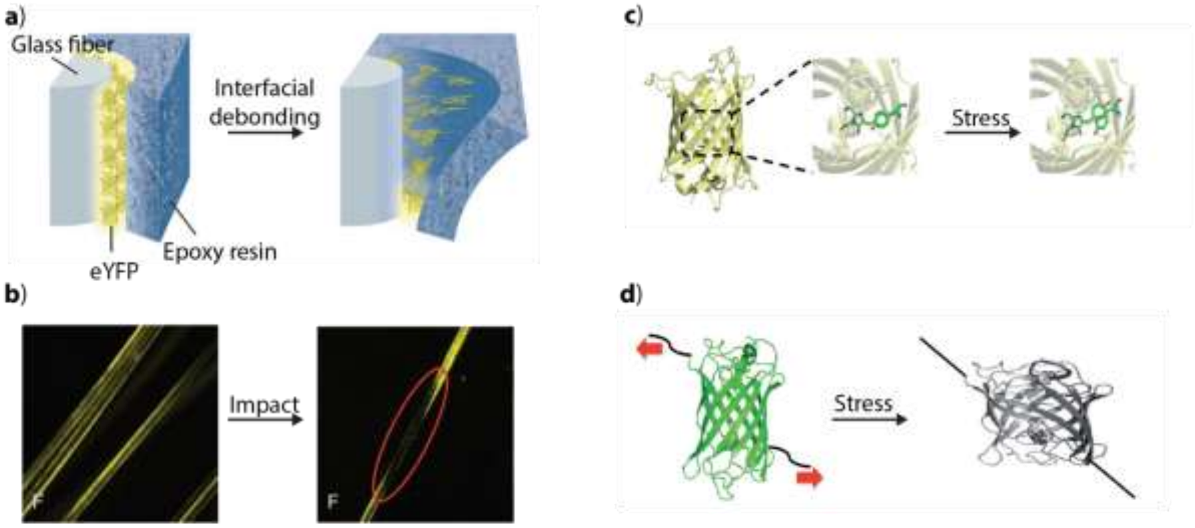

Figure 10. a) Working principle of the enhanced yellow fluorescent protein (eYFP) as mechanoresponsive motif at the interface between a glass fiber filler and an epoxy resin matrix. eYFP displays yellow fluorescence in the intact materials, while mechanical impact causes delamination and destroys the protein structure effectively quenching the eYFP fluorescence. b) Confocal fluorescence microscopy images of the fibers before and after impact testing show the initial and quenched fluorescence. Reproduced and adapted with permission.[53] Copyright 2013, Wiley-VCH. c) Illustration of the YFP that reacts to compression by a change in distance between its chromophore and a nearby arene group, which causes a hypsochromic shift in emission. d) Schematic

representation of GFP embedded in a PMMA matrix by radical polymerization. Compression causes fluorescence quenching due to the destruction of the GFP structure. Reproduced and adapted with permission.[153] Copyright 2014, Wiley-VCH.

These promising results certainly showcase the benefits of using relatively accessible fluorescent proteins in polymer matrices to create mechanochromic materials.[52] At the same time, however, the response is typically irreversible as the refolding of the protein into the original secondary structure is hindered in polymer matrices due to the lack of mobility. Moreover, it can be challenging to reliably detect the decrease of the fluorescence intensity in samples and a covalent incorporation of the protein into polymer matrices can be difficult. In this context, Longo and Jierry recently reported a modification of GFP with azide groups on opposite sides of the barrel-type secondary structure, which can be used to graft the protein onto alkyne-functionalized PDMS substrates by CuAAC.[152] When such samples were exposed to uniaxial tensile deformation, stretching up to 30% strain caused a reduction of the fluorescence intensity by up to 60%. In contrast to previous examples that exploited proteins, however, the fluorescence response was found to be reversible over three cycles of stretching and relaxation. However, strains beyond 30% could not be investigated due to failure of such samples. Further expanding the use of fluorescent proteins in polymer materials, Bruns and coworkers combined two fluorescent proteins that display a FRET process to elicit a mechanochromic response.[161] Thus, a protein-based mechanoresponsive motif was designed by covalently attaching an enhanced cyan fluorescent protein (eCFP) and an eYFP protein to the two cavities of a thermosome (THS), a chaperonin protein that assists folding amino acid sequences and serves to stabilize defined secondary structures. The THS protein holds the fluorescent eCFP and eYFP in close proximity to each other so that FRET can occur. This complex protein assembly (THS-eCFP-eYFP) was further modified with acrylate groups and incorporated into a poly(acrylamide) by free radical polymerization. In the pristine state, samples of the polymer containing the protein complex display an efficient FRET process from the eCFP donor to the eYFP acceptor. However, when micro-cracks were formed in the poly(acrylamide) matrix during tensile deformation, the FRET efficiency was observed to increase, presumably due to a shortening of the eYFP/eCFP distance.

The possibility to functionalize fluorescent proteins with many different functional groups, in principle allows for their incorporation as mechanoresponsive moieties into a wide range of polymer matrices. Moreover, the proteins already undergo a deformation of the fluorescent core at small strains, which immediately leads to a change in the fluorescence signal, while complete quenching of the fluorescence is observed at higher strains. Exploiting these different mechanisms can be anticipated to allow for a reversible and gradual sensing of a range of forces that are applied to a material, and the combination of multiple different proteins into a single material offers additional possibilities to tune the response. An improved understanding of the delicate relationship between the protein's secondary structure and the fluorescence signal will certainly further enable these approaches, and possibly aid in efforts to maintain the structural integrity of the proteins upon combination with polymer materials.

4. Mechanical Stimulation of Directional Supramolecular Interactions

With the exception of fluorescent proteins, the above-mentioned examples of non-sacrificial mechanoresponsive motifs encompass mechanisms that either rely on intramolecular conformational changes or non-directional interactions between dyes or dye pairs. The use of directional non-covalent interactions offers a means to precisely tailor the association between (macro)molecules.[32,40] In recent years, the exploration of the association between different types of directional binding motifs has led to an increased understanding of the assembly of molecular building blocks into higher-order structures, and more recent efforts have also explored how such directional non-covalent interactions can be used in the context of mechanoresponsive materials. In the following sections, reports that make use of metal-ligand

and host-guest interactions as mechanoresponsive moieties will be discussed, followed by an overview of selected examples that use hydrogen-bonding interactions in mechanoresponsive materials and highlight their potential utility for the development of mechanochromic polymers.

4.1. Organometallic Complexes as Mechanoresponsive Moieties

Metal-ligand (ML) complexes have garnered attention in the past decade as versatile non-covalent interactions that can act as mechanoresponsive motifs and produce various types of responses to mechanical deformation. Indeed, ferrocene (Fc) has been shown to behave as a mechanophore when covalently incorporated into high molecular weight polymer chains.[162,163] Sonication studies in solution have been carried out with Fc-containing polymers (*i.e.,* Fc-PMA, Fc-PU, and Fc-polybutadiene), and a faster decrease in molecular weight was observed for the polymers with organometallic linkages than for the reference polymers without. The organometallic complexes apparently dissociate in response to forces lower than those needed to cleave the covalent bonds of the polymer chain, and if KSCN, $K_4[Fe(CN)_6]$, or phenanthroline was present in the solutions of the Fc-containing polymers during sonication, the released Fe-ions formed red, blue, or purple complexes, respectively, thus translating the mechanochemical response into a visible color change.[162,163] A well-known class of motifs that directly yields mechanochromic organometallic complexes are bis- and terpyridine ligands that coordinate lanthanide or transition-metal ions via strong yet dynamic non-covalent bonds.[40] In these types of complexes, shortening metal-metal distances via mechanical stimulation leads to a red shift and broadening of the solid-state emission characteristics due to excimer formation.[164–166] For example, crystals or spin-coated thin films of Pt(II) complexes formed with a 1,3-di(2-pyridyl)-benzene (dpb) ligand change their dominant emission color from green/yellow to bright red upon grinding or rubbing, which XRD crystal analysis has linked to a reduction in the Pt–Pt distance to below 3.5 Å.[164–166] Such force-induced distortions of a crystal structure also occur for the chemically similar 2,6-bis(*N*-methylbenzimidazol-2'-yl)pyridine (Mebip) platinum(II) complex when dispersed in polymer matrices that are then subjected to damage or deformation. For example, blend films of a [Pt(Mebip)Cl](PF_6) complex (10–20 wt%) in PMMA, poly(ethyl methacrylate) (PEMA), poly(*n*-butyl methacrylate-*co*-isobutyl methacrylate) (PBMA-*co*-iBMA), or poly(butyl methacrylate) (PBMA) were prepared, and when these blends were subjected to scratching, compression, or extension, a change in the emission color from green to orange was observed due to the force-induced structural rearrangements that reduced the Pt–Pt distances (**Figure 11a**).[167]

If the tridentate, pyridine-based Mebip ligands are attached to the ends of a polymer chain, the addition of metal ions can furnish a cross-linked, supramolecular network that is endowed with the photophysical properties of its constituent ML complexes. For example, Weder and co-workers fabricated a metallosupramolecular polymer (MSP) assembled from a europium salt and a telechelic poly(ethylene-*co*-butylene) with Mebip ligands at the termini, which displays a strong red luminescence in solution due to the metal-centered emission. Ultrasonication of this MSP lead to a dissociation of the ML complexes and the concomitant loss of the characteristic metal-to-ligand-charge-transfer (MLCT) interactions significantly reduced the photoluminescence.[168] After sonication was stopped, the MSP re-assembled. Furthermore, when films of the Eu-MSP were imbibed with $Fe(ClO_4)_2$ by swelling in acetonitrile solutions containing this metal salt, sonication (ca. 15 min) or puncturing with a needle was sufficient to dissociate the Eu(III) complexes and allow Fe(II) to bind in its place. The more strongly bound Fe(II) complexes caused the previously colorless films to appear deep purple, accompanied by a precipitous drop in emission from the Eu-MLCT bands (**Figure 11b**).[168] Using a similar type of telechelic polymer, *i.e.*, a terpyridyl (Terpy)-end-capped four-arm poly(ethylene glycol) (4-arm-PEG), Holten-Anderson and co-workers fabricated a highly luminescent MSP gel that undergoes a sol-gel transition and changes its emission color in response to sonication.

Importantly, the process is reversible, with the blue-emitting fluid re-assembling into a white-emitting gel when left overnight.[48]

Miserez and co-workers took a different approach to exploit the mechanoresponsive nature of ML complexes and fabricated mechanochromic hydrogel composites with a double-layer design.[169] The composite featured different emitting species: carbon-nanodots (CDs) were incorporated into the top polyacrylamide hydrogel layer as covalent cross-links, while the bottom layer featured a polyacrylamide-*co*-polyacrylic acid hydrogel doped with lanthanide-ions that coordinated to the carboxylic acids as well as terpyridine ligands that furnished MLCT interactions (**Figure 11c**). The CDs and ML complexes in this composite were both efficiently excited when samples were irradiated with UV light (330 nm), but their respective emission maxima were observed at different wavelengths, *i.e.*, 414 nm (CD) and 544 nm (for Eu-complexes). As a result, the top layer displayed a blue CD emission, while the bottom layer with Eu-terpyridine complexes showed a red emission (green when Tb(III) was employed). Uniaxial tensile deformation of samples of this double-layer hydrogel up to 300% strain reduced the thickness of both layers in accordance with a Poisson’s ratio of ca. 0.5. However, only the upper-layer CD emission was significantly attenuated upon stretching the material, due to the difference in the absorption properties of the CD and ML complex constituents. Thus, the films displayed a strain-dependent decrease in the emission intensity ratio between the top and bottom layers (I_{414}/I_{544}), which was visually discernible as a change in emission color from yellow-green to blue-green (**Figure 11c**).[169]

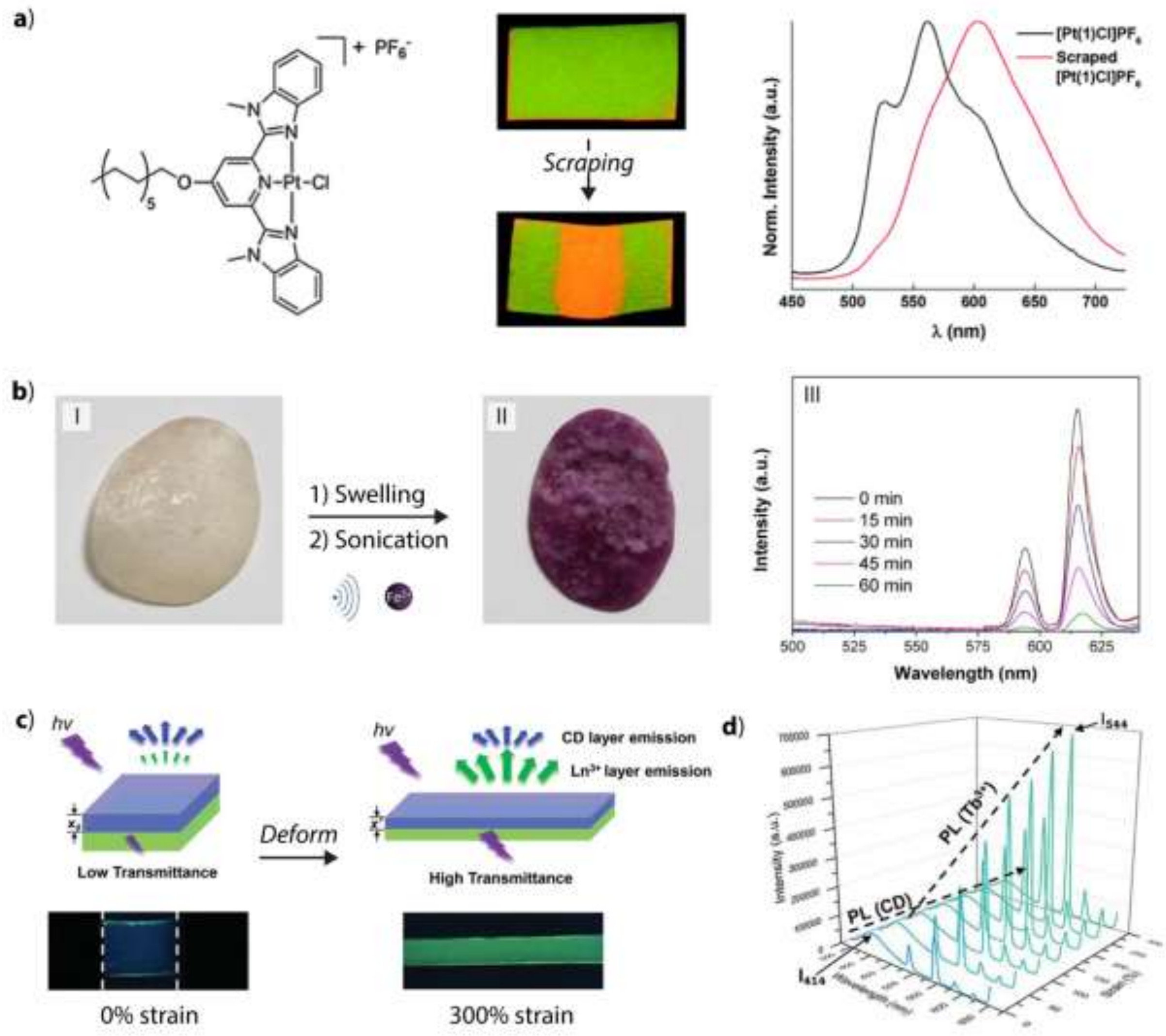

Figure 11. a) Chemical structure of a 2,6-bis(*N*-methylbenzimidazol-2’-yl)pyridine (Mebip) platinum(II) complex (left), photographs under UV illumination (365 nm) of filter paper onto which the crystalline complex was deposited before and after scraping (center), and fluorescence spectra (λ_{ex} = 377 nm) recorded of the filter paper before and after scraping (right). Reproduced and adapted with permission.[167] Copyright 2012, Royal Society of Chemistry. b) Photographs of a Mebip$_3$(Eu)-cross-linked metallosupramolecular polymer before [I] and after swelling in a solution containing Fe(ClO$_4$)$_2$, followed by sonication for 60 min [II]. [III] Solid-state fluorescence spectra (λ_{ex} = 365 nm) collected for the film in [I] after sonicating at different time intervals, showing a gradual decrease in emission originating from the Eu-metal-ligand charge-transfer band as a consequence of mechanically induced metal-ion exchange. Reproduced and adapted with permission.[168] Copyright 2014, American Chemical Society. c) Design of a double-layer mechanochromic hydrogel with a blue-light emitting upper layer consisting of carbon nanodots (CDs) incorporated into a polyacrylamide gel and a green-light emitting bottom layer comprising a polyacrylamide-*co*-polyacrylic acid gel doped with Tb^{3+}-ions and terpyridine ligands. Photographs of the hydrogel film before and after uniaxial tensile deformation to 300%. d) Evolution of the fluorescence spectra (λ_{ex} = 330 nm) of the film in (c) as a function of the applied strain. Reproduced and adapted with permission.[169] Copyright 2019, Wiley-VCH.

With the exception of this last example, the responses of mechanochromic materials with ML complexes is mediated by the intermolecular interactions between metal ions and ligand-functionalized polymers, allowing for a simultaneous control over both the optical and materials properties *via* the same motif. Alternatively, when transition metal-coordinating N-heterocyclic carbene (NHC) ligands are incorporated at the ends of a telechelic polymer, mechanically-induced dissociation of these catalytically active transition-metal complexes can be harnessed to produce chemiluminescence and a striking turn-on fluorescence.[26,170,171] For many decades, organometallic NHC complexes with Cu, Pd, or Ru, to name a few, have been employed as catalysts in a wide range of organic and polymerization reactions, the Grubbs second-generation catalyst being a prime example.[172] Catalyst activation is typically achieved using heat or an appropriate nucleophile, but ultrasound can also be used to mechanically activate NHC-complexes tethered to a polymer of sufficient molecular weight, and the metal and carbene species obtained upon dissociation of the complex can be used to signal the material's response. For example, Clough *et al.* incorporated Pd(bis-NHC) complexes at the termini of poly(THF) chains to form a MSP, the molecular weight of which decreased by half upon sonication due to breakage of the non-covalent NHC-metal linkages.[26] Once dissociated, the highly basic monocarbene ligands initiated decomposition reactions of adamantyl dioxetane and coumaranone derivatives that were present in solution, and the highly luminescent products of these reactions resulted in a striking turn-on mechanochromism.[26] Analogously, Binder and co-workers used imidazolium-terminated poly(isobutylene) (PIB) and polystyrene (PS) telechelic polymers to form Cu(bis-NHC)-containing MSPs. The latter were dissociated when exposed to ultrasound in solution, or when blends of the MSPs with poly(THF) were compressed; the Cu-monocarbene dissociation byproduct then activated a "click" reaction between azide and acetylene precursors that had also been embedded in the poly(THF) matrix, producing a highly fluorescent triazole compound.[170] Biewend *et al.* expanded on this work by covalently incorporating both the NHC complexes and fluorogenic precursors onto the termini of a polyurethane, and the as-prepared transparent PU films fluoresced bright blue in response to oscillating tensile forces applied by a rheometer.[171]

In addition to the capability of NHC complexes to produce a mechanochromic response via catalysis of ancillary reactions, crystals of Cu(bis-NHC) complexes themselves can also change their photoluminescent properties in response to temperature, exposure to analyte vapors, or grinding. The key to such a response is the counter-anion that stabilizes the positively charged complexes, and the distance of the counterion from the metal-center influences the excited state. For example, Hupp *et al.* ground single crystals of a di-copper $[Cu(bis\text{-}NHC)]_2$ complex weakly bound with two PF_6^- counterions and observed a red shift in the phosphorescence of the complex by nearly 200 nm, which changed its visible emission from weak blue to bright yellow.[173] Combining XRD and EPR measurements with DFT simulations, the authors captured structural changes in the complex that occurred as a result of the mechanical stimulation and concluded that the observed mechanoresponsive phosphorescent behavior arises from a shortening of the $Cu–PF_6$ distance, which distorts the excited-state coordination geometry from tetrahedral to trigonal.[173]

Analogous to these investigation with NHC complexes, Khusnutdinova and co-workers developed a series of photoluminescent iodo-copper pyridinophane (CuN_4-I) complexes (**Figure 12a**).[174] The emission color of the CuN_4-I complexes could be tuned by varying either the counterion or the bulkiness of the pendant groups attached to the pyridinophane, since these parameters influence the unique excited state geometries. The CuN_4-I complex was covalently incorporated into the hard segments of a polyurethane and the authors observed an increase in the photoluminescence (PL) intensity of the complex when the material was subjected to tensile deformation.[175] The emission wavelength remained unchanged, but the PL intensity increased in line with the applied stress above an onset of 5 MPa. The response was postulated to originate from the imparted restriction on the conformational switching of the pyridinophane ligand, which thus suppressed non-radiative relaxation pathways of the complex and enhanced its excited-state emission. Importantly, the stress-dependent PL enhancement of the PU(CuN_4-I) materials was reversible over six cycles and easily captured with a simple imaging setup to visualize the stress distribution in deformed films.[175]

The highly reversible response of intramolecular CuN_4-I complexes to deformation provides a valuable tool for monitoring mechanical stresses, but the relatively weak Cu-I bond renders the complex susceptible to degradation over time. Exchange of the iodine of the air-labile Cu–I coordinative bond for an NHC ligand allowed Filonenko *et al.* to effectively stabilize the Cu complexes against oxidation.[176] The pyridinophane component of the motif was then covalently linked into either the hydrogen-bonded hard phase or the polyether soft phase of a polyurethane, and subsequent complexation with Cu and the NHC ligand yielded the final, polymer-integrated complexes (referred to as Cu-HP or Cu-SP in the following; **Figure 12a**). When the Cu-HP and Cu-SP PU samples were subjected to tensile deformation up to stresses between 175–220 MPa at a strain rate of 5% min^{-1}, an increase in PL intensity of the samples was observed during extension, followed by a decrease in PL intensity while the samples relaxed under constant strain (**Figure 12b**). At this relatively slow deformation rate, stress dissipation in the PU materials appears to occur primarily *via* extension of the chains of the soft-phase and alignment of the hard-phase domains, both of which restrict conformational switching of the mechanoresponsive complex and thereby increases the fluorescence of the PU materials (**Figure 12d**, top path). The same deformation experiment carried out at a higher strain rate of 50% min^{-1} yielded different results; while the fluorescence response of Cu-SP mirrored the response at a low strain rate (**Figure 12b)**, the PL intensity of the Cu-HP material instead *decreased* during extension and subsequently *increased* logarithmically during stress-relaxation (**Figure 12c**).[176] The authors posit that the initial drop in intensity for Cu-HP at

50% min^{-1} was caused by a stress-dissipation mechanism that occurs at high strain rates in the PU matrix, namely breakage of hydrogen bonds in the hard phase and a concomitant reduction in conformation restriction of the complexes, followed by hard-phase reformation during relaxation which immobilizes them (**Figure 12d**, bottom path).[176] Finally, these mechanoresponsive complexes were also used as cross-linkers in poly(butyl acrylate) (PBA), and spectroscopic analysis of samples during deformation showed that stresses as low as 0.1 MPa could be detected, providing further evidence for the sensitivity of the organometallic complexes to mechanical stimuli.[177]

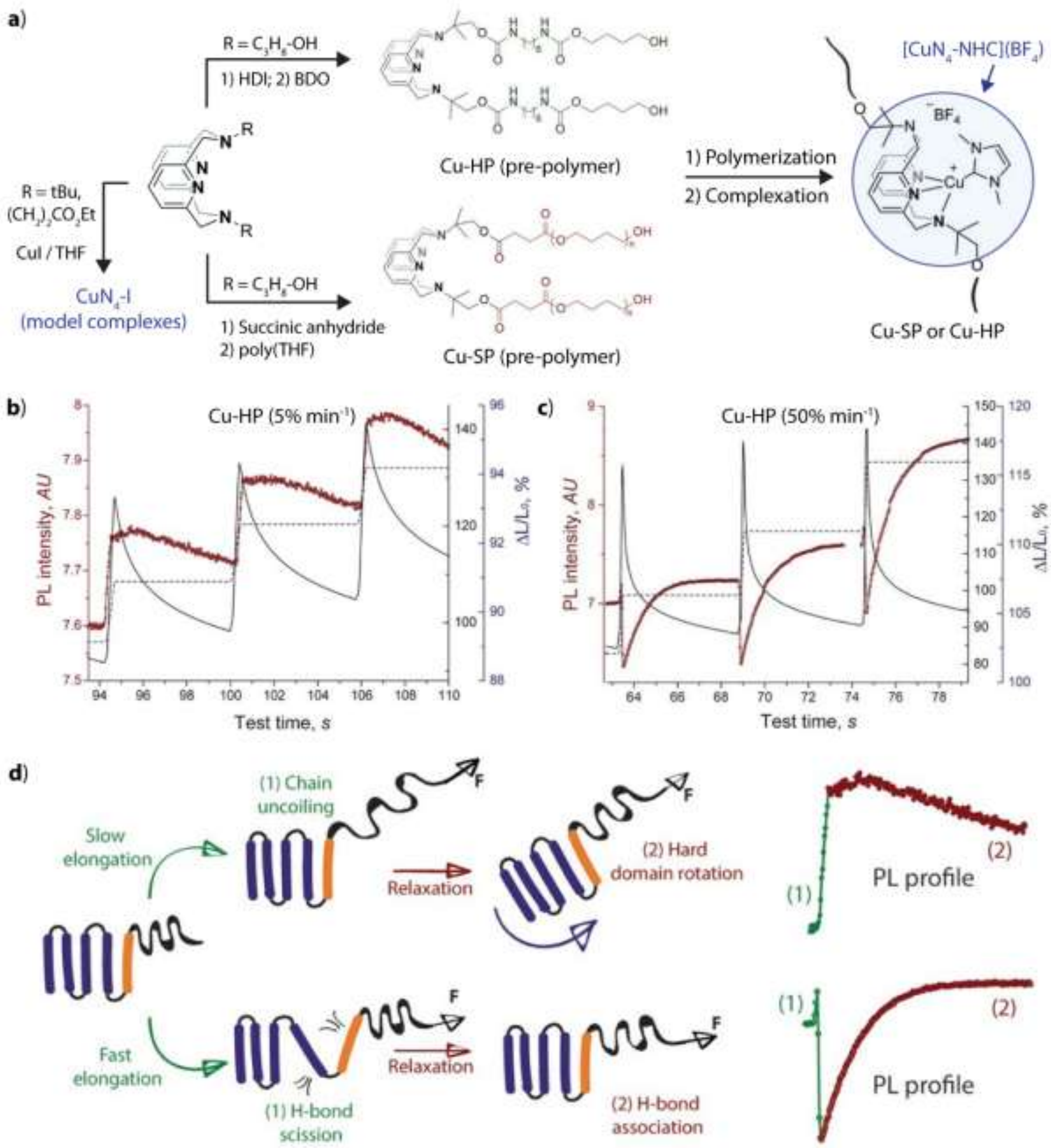

Figure 12. a) Synthesis of CuN_4-based mechanoresponsive organometallic complexes and their selective incorporation into soft and hard domains of a polyurethane (PU). b,c) Change in photoluminescence intensity (red points) of PU films with the copper complexes in the hard phase as monitored during stepwise extension-relaxation testing (applied strain shown as blue dashed lines; stress-time curves shown as black lines). For each step, the samples were elongated at 5% min^{-1} (b) or 50% min^{-1} (c) and subsequently allowed to relax under constant strain before re-extension. d) Schematic depiction of the proposed mechanisms of stress-dissipation that occurs in PU films at different strain rates. Reproduced and adapted with permission.[174,176] Copyright (a) 2017, Royal Society of Chemistry; Creative Commons CC BY license (a-d) 2018, Wiley-VCH.

Moreover, the emission wavelength of [CuN_4-NHC](BF_4) was successfully tuned by modifying the excited state geometry, *i.e.*, by employing an NHC ligand with bulky diisopropyl (DIP) moieties.[178] Polyurethanes in which this complex was covalently integrated responded to tensile elongation by an increase in PL intensity as well as a blue shift of the emission band, which was attributed to an increasing separation of the BF_4^- counterion from the complex as the surrounding polymer matrix deformed. While the increase in PL intensity correlated closely with the applied stress, the emission intensity ratio (I_{530}/I_{610}) was observed to increase more rapidly, especially at high strains, and a plateau was reached once strain-induced crystallization set in, a process the authors monitored by FTIR spectroscopy.[178] Taken together, the findings with pyridine- and NHC-based organometallic complexes show that both inter- and intramolecular metal-ligand interactions can be used in materials to generate striking fluorescence responses to mechanical stimuli, which can be in turn used to elucidate complex material deformation processes that are otherwise difficult to observe in real-time.

4.2. Host-Guest Complexes as Mechanoresponsive Motives

The cooperative assembly of two (or more) molecules can give rise to host-guest complexes, which often consist of inclusion complexes featuring a guest that resides in the cavity of a host. The formation of such complexes is frequently driven by multiple different types of non-covalent interactions, *e.g.*, hydrogen bonding and dispersive van der Waals or hydrophobic interactions. The typically cooperative influence of these different contributions to molecular association is described as host-guest interactions. The corresponding host-guest complexes are common motifs in supramolecular chemistry and their response to mechanical stimuli has been often studied by SMFS to determine specific rupture forces.[179] Particular attention has been paid to the interactions between *β*-cyclodextrin as the host and ferrocene or adamantyl guests,[180–183] as well as the interactions between cucurbituril as the host with an adamantly guest.[58,184] The studies revealed that a single *ß*-cyclodextrin/ferrocene complex has a lower rupture force of ca. 55 pN[182,183] than a single *ß*-cyclodextrin /adamantyl complex (102 pN).[180] Depending on the employed loading rate, the cucurbit[7]uril/adamantyl complexes reportedly rupture at forces of 95 to 140 pN,[184] while cucurbit[8]uril/adamantyl complexes are already disrupted at force of only 39 pN.[58]

These studies on individual host-guest complexes suggest that these can be broken by mechanical forces, however thus far only few mechanochromic materials based on host-guest interactions have been reported.[46,54] Recently, Dalcanale and coworkers employed a host-guest complex as a non-covalent cross-linking agent that renders a polymer mechanochromic (**Figure 13a**).[54] To this end, the authors prepared a complex using a tetraphosphonate cavitand as the host (bearing four double bonds for incorporation into the polymer) and a pyrene-conjugated, *N*-methylated pyridinium salt (bearing one double bond) as the guest. The complex was formed in DCM and was added to a mixture containing vinyl terminated PDMS. Subsequent curing allowed for the incorporation of the host-guest complex as a supramolecular cross-linker into the PDMS matrix. Films of this material exhibited no fluorescence in the relaxed state, since the emission from pyrene was completely quenched in the host-guest complexes. Imaging samples of the PDMS film under UV light illumination during tensile deformation showed that the pyrene fluorescence was discernible when the sample was stretched and after breakage, indicating that the host-guest complex was disassembled through the applied strain. A similar turn-on response was also observed during three-point bending tests with notched samples, where the highest fluorescence intensity could be observed in highly stretched regions of the sample around the propagating crack tip.

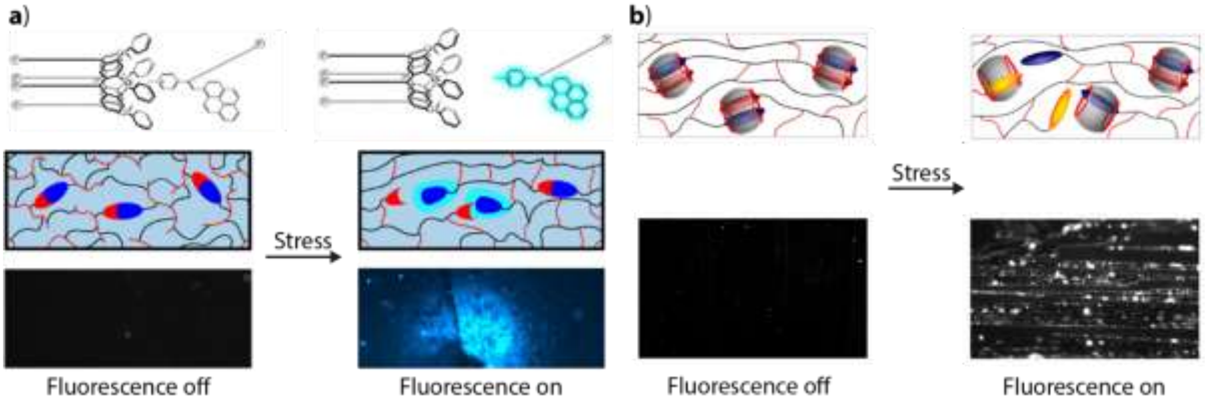

Figure 13. Examples of polymers that feature host-guest complexes as mechanoresponsive motifs. a) Chemical structure (top) and schematic depiction (middle) of complexes between a tetraphosphonate cavitand host and a pyrene-conjugated, *N*-methylated pyridinium salt guest. The complex was incorporated as a supramolecular cross-link in poly(dimethylsiloxane) and the pyrene fluorescence is switched on when the complex is disassembled upon mechanical deformation of the polymer, as seen in fluorescence microscopy images (bottom) taken before and after deformation. Reproduced and adapted with permission.[54] Copyright 2017, American Chemical Society. b) Schematic (top) of a carbon fiber reinforced epoxy resin containing a ternary host-guest complex composed of a cucurbit[8]uril host and perylene monoimide as well as azobenzene or dibenzofuran as guests. The pyrene-based fluorescence of intact complexes is quenched, but mechanical stresses disassemble the complexes, and fluorescence is observed, *e.g.*, in fluorescence microscopy images (bottom) before and after fatigue testing over 100000 cycles. Reproduced and adapted with permission.[46] Copyright 2019, American Chemical Society.

In a similar manner, ternary host-guest complexes that use cucurbit[8]uril as the host for a combination of fluorophore and quencher moieties as guests were employed to prepare mechanochromic polymer materials (**Figure 13b**).[46] Cucurbit[8]uril can form stable ternary host-guest complexes in which both a perylene monoimide fluorophore and an azobenzene or dibenzofuran quencher moiety are simultaneously accommodated as guests in polar environments. In the complexed state, the perylene fluorescence is thereby effectively quenched by the host. To integrate such ternary host-guest complexes into polymer materials, fluorophore and quencher moieties that feature an amine functional group were prepared, the complex with cucurbit[8]uril was formed, and the assembled host-guest complex was used as a cross-linking reagent for the preparation of a carbon fiber-reinforced epoxy resin. During compression and tensile deformation of such composites, a fluorescence increase was observed above a threshold strain of ca. 70%, indicating the disassembly of the host-guest complexes. To test the material's fatigue behavior, tensile tests up to 60% strain were performed by consecutive application of 1000–100,000 loading and unloading cycles. In the high-cycling range (*i.e.,* close to 100,000 cycles) the stiffness of the material dropped, which resulted in a lowerering of the threshold strain for the disassembly of the host guest complexes and a gradual fluorescence turn on was accordingly observed.[46] These recent examples showcase that host-guest complexes provide a very interesting platform for the development of novel types of non-covalent mechanoresponsive motifs that can translate an applied mechanical stimulus into a discernible response, even in complex materials such as stiff and fiber-reinforced polymer composites.

4.3. Hydrogen Bonding Interactions as Mechanoresponsive Motives

Hydrogen bonding interactions are certainly among the most widely explored binding motifs in supramolecular chemistry,[185] and many investigations have explored the mechanical stability of hydrogen bonding interactions and demonstrated that they are susceptible to break when exposed to mechanical stresses. This has, for example, been demonstrated by single-molecule force spectroscopy (SMFS) experiments that were used to determine the forces required to rupture, *e.g.*, polymers with complexes of quadruple hydrogen-bonding ureido-4[1H]-pyrimidinones (UPy) or benzene-1,3,5-tricarboxyamide (BTA) interactions,[186] hydrogen-bonded coiled-coil domains of proteins,[138,187] DNA base pairs,[188] as well as more complex DNA origami tubes with Holliday junctions (DNA cross-links),[189] to name a few. At the same time, however, relatively few studies have investigated the use of hydrogen bonding interactions as distinct responsive motives for the preparation of mechanochromic polymer materials. A notable exception is the above-discussed study by Walther and coworkers that demonstrates that mechanochromic materials can be obtained when hydrogen bonding DNA double strands are used in combination with suitable chromophores (*vide supra*).[45]

Biomacromolecules such as the natural muscle protein titin display intricate mechanoresponsive behaviors, and the following brief discussion of artificial hydrogen-bonded polymers that mimic the natural protein may serve to highlight the great potential of hydrogen bonding interactions for use as mechanoresponsive motifs. Titin comprises unstructured protein domains that alternate with folded immunoglobulin domains; when subjected to mechanical force, the unstructured domains extend first, followed by an unfolding of the structured domains at higher forces.[190] The ability of titin to dissipate mechanical forces in such a sequential manner endows muscle tissue with its high strength, stability, and resilience.[190] Examples that have aimed to mimic such responses to mechanical stimuli in artificial polymers include the efforts by Guan and coworkers, who designed a polyurethane composed of domains of soft poly(THF) and molecular loops that were held together by pairs of associating quadruple hydrogen-bonding UPy motifs (**Figure 14a**).[191] The response of the artificial UPy-containing polymer was explored by AFM-based SMFS experiments. The recorded force extension curves showed a clear saw-tooth pattern upon straining the polymer that originated from the consecutive rupture of three different types of UPy dimers at 100 pN (head-to-tail) or 200 pN (tail-to-tail and head-to-head) along the polymer backbone. Each rupture event was accompanied by an increase in polymer chain length and subsequent relaxation until the extended contour was again reached, mimicking the response of the natural protein. In addition to the molecular-level investigations, the properties of such hydrogen-bonded polymers were also explored in bulk,[191] and the mechanical characterization showed that the polymers with intermolecular UPy dimer loops displayed a higher strength, toughness, and elasticity than reference polyurethanes. Akin to the natural protein, the polymers with UPy loop units were found to completely recover the original properties after relaxation. Furthermore, quadruple hydrogen bonding motifs were incorporated into "double-closed" loop structures and integrated into polymers to more closely mimic the uniformity of the response of titin to mechanical deformation (**Figure 14b**),[192–194] and further iterations on the design of such motifs incorporated bulky substituents that block non-specific interactions between UPy dimers.[195]

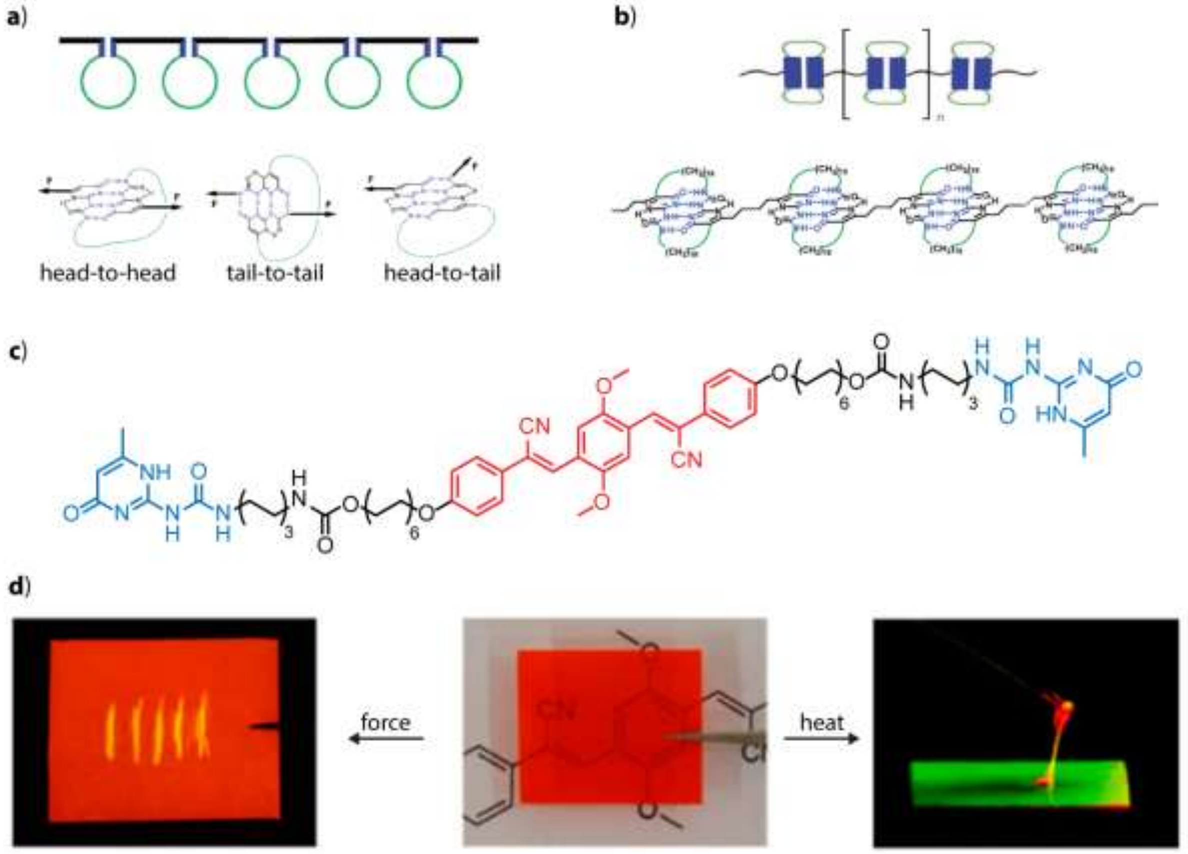

Figure 14. a) Schematic depiction of a loop structure featuring multiple complementary ureido-4[1H]-pyrimidinone (UPy) as a titin-inspired hydrogen bonding motif and the different binding modes displayed. Reproduced and adapted with permission.[191] Copyright 2004, American Chemical Society. b) Depiction of a polymer system that makes use of UPy double closed loop structures as responsive hydrogen-bonded motifs in the polymer backbone. Reproduced and adapted with permission.[193,194] Copyright 2007, 2009 American Chemical Society. c) Molecular structure of a UPy-functionalized cyano-OPV (UPy-OPV-UPy). d) Images of UPy-OPV-UPy films under ambient lighting (center), and under UV illumination (365 nm) after scratching (left) and upon heating (right). Reproduced and adapted with permission.[196] Copyright 2017, American Chemical Society.

The preceding examples highlight the intricate responses hydrogen bonding motifs can display upon mechanical stimulation, but the disruption of the non-covalent interactions is in these cases not accompanied by an optical signal. To achieve a mechanochromic response, Weng and coworkers combined covalent mechanophores with such non-covalent mechanoresponsive motifs.[197] The authors prepared a polyurethane that features UPy hydrogen bonding motifs and a covalent spiropyran mechanophore as co-monomers. The spiropyran activation, namely the electrocyclic ring opening reaction from a colorless spiro-form to a colored merocyanine form upon mechanical stimulation, was found to occur at higher strains (550%) and stresses (11 MPa) than in the non-UPy bearing polymer (450%, 6.9 MPa). An analysis by small angle X-ray scattering suggested that UPy dimers need to break in prior to the strain-induced activation of the spiropyran.[197] Subsequently, the same group also prepared short polyurethane macromonomers with spiropyrans in the backbone that were end-functionalized with UPy motifs. Mechanical testing of films of the supramolecular polymer revealed tangible mechanical properties, and the spiropyran activation in response to mechanical deformation was enhanced by a factor of 4-5 in comparison to a polymer without the hydrogen bonding UPy linkages.[198]

Exploiting the non-covalent association of aggregachromic OPV dyes to elicit an optical signal, Lavrenova *et al.* reported the preparation of a hydrogen-bonded mechanochromic material.[196] To achieve this, a supramolecular monomer was prepared that contained an aggregachromic cyano-OPV moiety at its center and UPy-groups at the two termini. This building block self-assembled to form a glassy supramolecular polymer (UPy-OPV-UPy). Melt-processed samples displayed appreciable mechanical properties and fluoresced red, indicating that the hydrogen bonding facilitated chain extension and that the OPV moieties adopt arrangements that support excimer emission. A pronounced change of the fluorescence color to yellow was observed when films of this material were scratched or fibers were cut, indicating that excessive mechanical force is capable of altering the structure so that the electronic interactions among the OPV motifs change. Moreover, melting the material (ca. 140 °C) completely disrupted the dye aggregates as indicated by a shift of the emission from red to green. After cooling to room temperature, the initial red emissive state was restored,[196,199] and the reversible and dynamic binding between the UPy motifs enabled a facile processing of the material into various shapes.

Tremendous progress has been made regarding the incorporation of hydrogen-bonding interactions as mechanoresponsive moieties in polymer materials. However, a majority of the investigations have focused on fundamental studies by means of SMFS experiments on individual polymer chains. Even though recent studies indicate that the dissociation of hydrogen bonding motifs in bulk polymer materials can be useful to tailor the mechanical properties and the chromic responses of mechanophores or aggregachromic dyes have been combined with hydrogen bonding interactions, there have, to the best of our knowledge, so far not been any reports of systems in which the dissociation of binding motifs *concomitantly* provides a readout, such as a fluorescence or visual color change,[200] that would allow for the detection of bond formation or breakage events without the need for the highly advanced equipment used in SMFS experiments. Combining these two functionalities could serve as an intriguing starting point for the development of new types of non-covalent mechanophores.

5. Chromic Responses to Conformational Changes of Conjugated Macromolecules

Simple conformational changes on a molecular level and changes to the intermolecular distance can afford chromic responses, and many intriguing examples of such systems have been discussed in the preceding chapters. However, it can be difficult to transfer macroscopic stresses that are applied through bulk mechanical deformation in an efficient manner to responsive molecular entities. To achieve such an effective force transduction, the molecular moieties are frequently covalently attached to or blended with a polymer, and the deformation of the polymer chains evokes the desired molecular-level changes. Instead of relying on these transduction mechanisms to endow materials with a mechanochromic behavior, changes to an individual polymer chain can also be exploited. Polymer chains undergo conformational changes when subjected to mechanical force, such as stretching and uncoiling motions that involve bond rotations, the adjustment of bond angles, and changes to bond lengths, before bond rupture ultimately occurs.[201] The understanding of these motions, which are difficult to observe directly, is primarily derived from polymer theory and molecular dynamics simulations. In some polymers, the changes in conformation are directly linked to changes in physicochemical properties. For example, the optical properties of conjugated polymers are intrinsically linked to the length of the segments across which electron delocalization can occur, *i.e.*, the effective conjugation length.[202] The latter can increase when a polymer is stretched and the conjugated segments along the backbone align to each other; conversely, a distortion of the backbone can lead to a disruption of the conjugation and reduces the effective conjugation length. The increase or decrease of the length of fully conjugated segments directly changes the absorption and emission properties of such polymers, and the conformational changes caused by mechanical deformation may, hence, directly furnish an optical signal. A plethora of conjugated polymers have been developed,[203] and many of these polymers could perhaps be used as mechanochromic materials.[9] To illustrate how mechanical deformation can lead to optical signals as the conjugation length increases, examples of conjugated polyelectrolytes and poly(thiophene)s will be introduced in greater detail in the present review, while poly(diacetylene)s will be discussed as illustrative examples that showcase how an optical signal is obtained as mechanical deformation disrupts the conjugation in polymers.

Polyelectrolytes with pendant ionic groups, such as SO_3^-, CO_2^-, PO_4^{2-}, or NR_3^+ and a conjugated polymer backbone are generally interesting because they are soluble in polar solvents like water.[204] To prepare conjugated polyelectrolytes, monomers such as dioxaborolane-substituted fluorene bearing alkyl bromide pendant groups and 4,7-dibromo-2,1,3-benzothiadiazole are typically polymerized in a cross-coupling based polycondensation reaction, and a subsequent post-polymerization modification step is then used to introduce the desired ionic groups.[204] Following this general strategy, Sprakel and coworkers recently reported the preparation of a poly[9,9′-bis(3′-propanoate)fluoren-2,7-yl] sodium salt (PF3) by

Yamamoto coupling and demonstrated its utility for eliciting a chromic response to mechanical deformation.[49] PF3 was co-assembled with a neutral-cationic diblock polypeptide, consisting of a zwitterionic and a hydrophilic, stabilizing coil block of 400 amino acids, into a ribbon like structure. In aqueous solutions, the electrostatic interactions between the cationic lysine groups of the polypeptide and the anionic carboxylate groups of PF3 forces conjugated backbone of the latter into a stretched conformation with reduced rotational degrees of freedom, which manifested in a bathochromic shift of the absorption band (3 nm) as well as a significant change in the ratio of the vibronic transitions in the corresponding fluorescence spectra. The change in the vibronic transitions was found to linearly depend on the grafting density, which is defined as the number of side grafts of diblock polypeptide per unit length of the backbone, up to 0.14 nm^{-1}. Above this threshold, the PF3 was fully stretched and no further response was observed, even though charge compensation was not reached. Changing the ionic strength of the aqueous solutions through addition of sodium chloride was found to completely reverse the changes in the UV-Vis and fluorescence spectra as the coulomb interactions between PF3 and the polypeptide were disrupted.[49] Moreover, the monomer 2,7-dibromo-9,9-bis(3-(*tert*-butyl propanoate))fluorene was co-polymerized with 4-bromo-2,1,3-benzothiadiazole and subsequent deprotection of the carboxylic acid groups yielded a co-polymer (PF3-BT, **Figure 15a**).[205] In the latter, the benzothiadiazole moieties act as FRET acceptors that reside in the polymer's backbone. When solutions of poly(*N*-methyl-2-vinylpyridine-*co*-ethylene oxide) were added to solutions of this PF3-BT polymer, the electrostatic interactions between the cationic *N*-methyl-2-vinylpyridine block and the carboxylic acid groups of PF3-BT led to the formation of a single PF3-BT-containing assembly, causing planarization of the backbone and a change in the intensity ratio of the three vibronic maxima in the emission spectra. When the ratio of anionic PF3-BT and cationic poly(*N*-methyl-2-vinylpyridine-*co*-ethylene oxide) exceeded a certain threshold, interchain FRET occurred and BT emission became more pronounced, indicating the formation of multimolecular micelles (**Figure 15b**). Furthermore, PF3 and PF3-BT co-assemblies with more complex viromimetic proteins was used to gain a deeper understanding of the mechanism of virus capsid formation.[206] In these examples mechanical deformation is not applied macroscopically, but rather *via* coulomb interactions. Despite the fact that the forces applied cannot be measured (in the sense of a stress), the described conjugated polymers still readily function as sensors of the deformation of the chains.

The same group designed a conjugated co-polymer (FS1) comprising poly(fluorene-*alt*-benzothiadiazole) (F8BT) as the donor backbone doped with dithienyl benzothiadiazole (DTBT) co-monomers as acceptors, which can undergo intramolecular FRET ($R_0 = 4.9$ nm), and applied it as a single macromolecular strain sensor (**Figure 15d**).[22] Thus, the conjugated polymer was blended at very low concentration in a polystyrene film and subjected to uniaxial tensile deformation above the T_g (105 °C) of polystyrene. Subsequent cooling below T_g led to fixing of the strained chain conformation. The samples were analyzed by single-molecule emission spectroscopy, where individual conjugated polymer chains were excited with a 405 nm laser and the emission was detected with a hyperspectral camera. Starting from 70%, the FRET efficiency decreased with increasing strain and a force detection threshold for the system was computed to be ~300 fN (**Figure 15c**).[22]

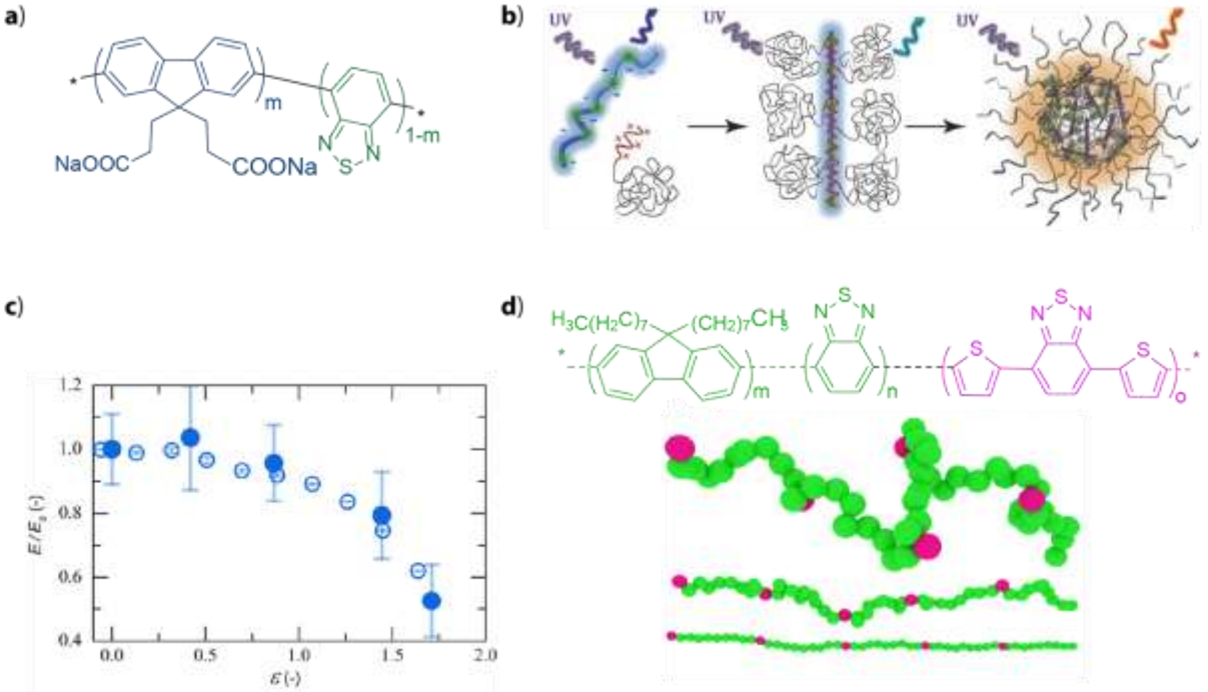

Figure 15. a) Chemical structure of a co-polymer of a fluorene derivative and a benzothiadiazole derivative (PF3-BT) and, (b) illustration of its co-assembly with poly(*N*-methyl-2-vinylpyridinium)-*b*-poly(ethylene oxide) first into a monomolecular PF3-BT (blue chains) containing complex, and then into multimolecular micellar structures. Reproduced and adapted with permission.[205] Copyright (a,b) 2016, Wiley-VCH. c) Change of the Förster resonance energy transfer (FRET) ratio with increasing strain as determined experimentally (closed circles) and computationally (open circles) with a conjugated co-polymer of poly(fluorene-*alt*-benzothiadiazole) and dithienyl benzothiadiazole co-monomers (FS1). d) Chemical structure of the FS1 copolymer and schematic illustration of the conformational changes that occur upon tensile deformation. Reproduced and adapted with permission.[22] Copyright (c,d) 2018, Elsevier, Inc.

Changes in the effective conjugation length in response to applied mechanical forces have also been exploited in poly(alkyl thiophenes) such as poly(3-dodecylthiophene),[207] poly(3-hexyl-thiophene),[208] and poly(octylthiophene).[209] When compressive stresses are applied to samples of these polymers a bathochromic shift in the absorption and emission spectra is observed, which correlates with a straightening of the polymer backbone and an increase in conjugation length. Direct monitoring of changes in the photophysical properties can be difficult in pure polymers. Moreover, conjugated polymers often display inferior mechanical properties. However, blends of PMMA containing poly(3-octylthiophene) (P3OT) or poly(3-hexyl-thiophene) (P3HT) can be prepared to investigate the responses upon mechanical deformation.[210,211] In one study 0.05–1.0 wt% of P3OT was added to PMMA and the samples were subject to uniaxial tensile formation while simultaneously measuring the fluorescence lifetime. A stark decrease of the lifetime (490 to 406 ps) was observed when the PMMA/P3OT blend was deformed in the elastic region of the stress-strain curve, while the lifetime increased and plateaued at 440 ps upon plastic deformation of the sample. Similar results were also reported for samples of a PMMA/P3HT (0.05 wt%) blend that were subjected to tensile deformation.[210] These findings suggested that the conjugated polymer backbone was distorted upon mechanical deformation, and steady-state fluorescence spectra showed that plastic deformation caused a red shift of the material's fluorescence, indicating that an increase in the polymer's conjugation length occured.[210]

More recently, similar blends of conjugated polymers with a non-conjugated polymer matrix were prepared with the hydrophilic poly(3-tri(ethylene glycol)thiophene) (P3TEOT) and polar poly(vinyl alcohol) (PVOH) as the matrix.[50] Tensile deformation of samples of a PVOH/P3TEOT (1.35 wt%) blend above the T_g (75 °C) of the matrix caused a shift in the absorption band in the UV-Vis spectra from 460 to 510 nm, a shift of the emission band from 600 to 615 nm, and a visually discernible color change from orange to red (**Figure 16**). Micrographs taken with crossed polarizers during stretching of samples to 100% strain reveal that the P3TEOT aligned in the stretching direction, a process that could be reversed by heating the sample. Moreover, the characterization of such blends indicated a concentration-dependent mechanochromism: at concentrations of P3TEOT above 0.01 wt%, tensile deformation of samples of blends with PVOH led to a bathochromic shift in the UV-Vis and fluorescence spectra, which was interpreted as an increase in conjugation length and an intermolecular alignment of the P3TEOT chains. When P3TEOT was blended with PVOH in a concentration range of 10^{-2} to 10^{-4} wt%, tensile deformation furnished a hypsochromic shift of the maximum in the fluorescence spectra, while the UV-Vis spectra remained unchanged. These findings were ascribed to the presence of smaller, less extensive stacked, and less rigid P3TEOT aggregates, which did not extend isotropically in response to tensile deformation so that no increase in conjugation length was discernible. At even lower P3TEOT concentrations of ca. 10^{-5} wt%, no distinct changes to the photophysical properties were observed upon tensile deformation of films, presumably due to lack of intermolecular interaction and distortion of individual, molecularly dissolved chains.[50] The concentration-dependent study suggests that the interchain packing of the conjugated polymer is decisive when aiming to change its conformation and thereby alter the photophysical properties. The properties of the conjugated polymer additive, its concentration, as well as the mechanical properties of the matrix, hence, need to be considered for the preparation of mechanochromic materials.

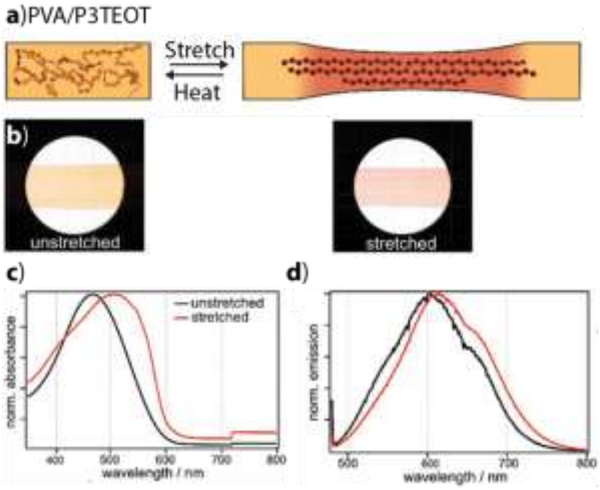

Figure 16. a) Schematic illustration of the deformation of samples poly(vinyl alcohol) (PVOH) into which poly(3-tri(ethylene glycol)thiophene) (P3TEOT) was blended. The P3TEOT chains align upon uniaxial tensile deformation of samples. b) Photographs of pristine and stretched samples of a PVOH/P3TEOT (1.35 wt%) blend show the color change from orange to red upon deformation. c–d) Comparison of the (c) UV-vis and (d) fluorescence spectra of the pristine (black) and stretched (red) samples of the PVOG/P3TEOT (1.35 wt%) blend. Reproduced and adapted with permission.[50] Copyright 2019, Wiley-VCH.

The distortion of a polymer's backbone can also furnish a chromic response, as prominently observed in the response of poly(diacetylene)s (PDAs) to mechanical stresses.[212,213] The conjugated polymers can exhibit mechanochromism when the conformation of the backbone is perturbed, and a decrease in the conjugation length is generally observed that causes a distinct color change of PDAs from blue to red.[212] The polymer can be prepared by the assembly of the diacetylene-based monomers at interfaces or in hydrogen bonded-assemblies, amongst others, followed by a topochemical polymerization initiated by UV irradiation or heating.[214] The pristine PDA polymers have been frequently reported to display a mechanochromic response upon grinding, shearing or swelling.[212,215]

More recently, PDAs have been developed that display a mechanochromic response that can be reversed upon heating the material.[216] To this end, a monomer was prepared in which two diacetylene-bearing alkyl chains were connected *via* an amide bond with a diphenyl disulfide moiety in the center of the structure (**Figure 17a**). After the two-fold topochemical polymerization of the diacetylenes into a ladder-type PDA, hydrogen bonding between the amide groups and π-interactions between the phenyl groups was expected to stabilize the structure. Indeed, grinding-induced distortions of the polymer led to a disruption of the backbone, as indicated by a color change from blue to green, which could be reversed by heating to 140 °C followed by cooling to 25 °C, effectively recovering the initial state with a blue-colored PDA (**Figure 17b**). Additionally, the chromic changes have been coupled to a fluorescence switch-on response by utilizing alkyl chain-bearing diacetylene monomers connected to a tetrazine fluorophore.[217] After polymerization by UV irradiation at 254 nm, the polymer resides in the blue form, and the tetrazine fluorescence is quenched by energy transfer to the PDA backbone. Upon grinding of the polymer or compression with an AFM tip, however, the polymer backbone was distorted and energy transfer hindered, which resulted in a bright fluorescence of the tetrazine.[217]

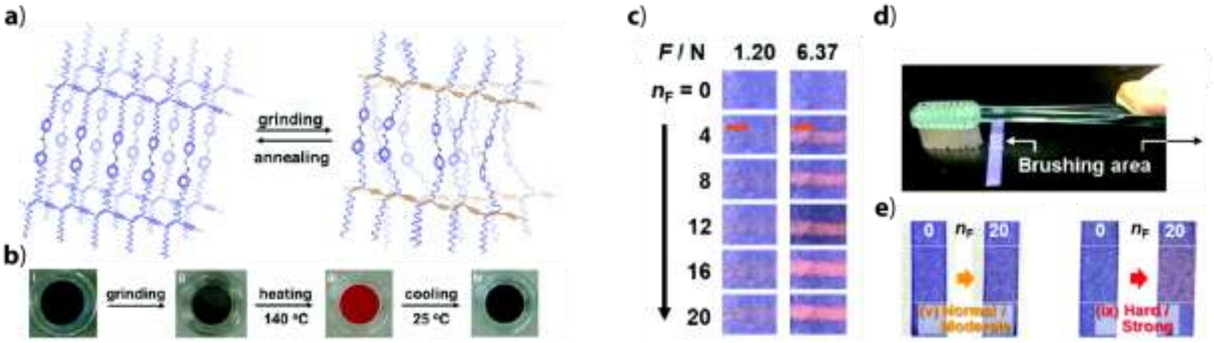

Figure 17. a) Schematic depiction of the reversible structural rearrangements during grinding of a ladder-type, two-fold poly(diacetylene) in which hydrogen-bonding as well as π-interactions enable the reversibility of the chromic response. b) Photographs of samples of the polymer shown in (a) taken before and after grinding as well as after heating to 140 °C and subsequent cooling to 25 °C, which effectively restores the optical properties of the pristine material. Reproduced and adapted with permission.[216] Copyright (a,b) 2019, Royal Society of Chemistry. c) Color change of paper strips that were imbibed with a poly(ethylene imine)/poly(diacetylene) blend before and after repeatedly applying frictional forces of 1.2 or 6.4 N. d) Experimental setup for determining the brushing force of a toothbrush with the poly(ethylene imine)/poly(diacetylene) paper strips. e) Photographs of the paper strips before and after brushing 20 times with a normal or hard toothbrush while applying moderate or strong forces to the surface. Reproduced and adapted with permission.[218] Copyright (c-e) 2020, Royal Society of Chemistry.

Furthermore, composite materials and polymer blends have also been developed that utilize the PDA as a colorimetric probe. For example, Rubner *et al.* used different diacetylene derivatives (2,4-hexadiyne-l,6-diol or 5,7-dodecadiyne-1,12-diol) as hard segments in the synthesis of linear polyurethanes.[59] During solvent casting of the polymer the diacetylene groups self-assembled, and subsequent annealing of samples at 90 °C induces the polymerization into PDAs. Tensile deformation of such samples up to ca. 600% strain induces a gradual color change from blue to red, which correlated with a shift in the main absorbance band from 625 to 470 nm. Moreover, a blend of a paraffin wax and the PDA poly(10,12-pentacosadiynoic acid) was prepared that was used as a crayon for drawing on paper.[43] Drawing with the crayon deposited the wax/PDA blend as a blue-colored solid, but shearing the paper by rubbing with a finger induced a color change from blue to red.

In another recent example, a diacetylene monomer (10,12-pentacosadiynoic acid) was blended with poly(ethylene oxide) as a matrix and wires of the polymer blend with diameters between

50 and 5000 nm and lengths of up to tens of millimeters were manually drawn from a viscous chloroform across a tuning fork.[219] The shear forces during the drawing process were found to lead to an alignment of the diacetylene monomers, and polymerization into PDA was successfully achieved by UV irradiation (λ = 254 nm). Mechanical forces were then applied to the wires through oscillations of the tuning fork, which was found to be sufficient to induce a color change from blue to red.[219] The high sensitivity of the chromic response of PDAs was recently also demonstrated by Park *et al.* in an investigation that used poly(dimethyl siloxane)/PDA blends.[220] The latter were swollen into organogels by exposure to a mixture of saturated aliphatic hydrocarbons, and the swelling process was sufficient to deform the PDA backbone and induce a color change from blue to red. A detailed investigation of the process showed that the intensity and speed of the color change correlated with the chain length of the employed aliphatic hydrocarbons, which allowed for a differentiation between samples of diesel fuel and a composition that additionally contained kerosene (a common illegal practice to tamper diesel). Furthermore, the assembly between 10,12-pentacosadiynoic acid and different alkylamines or poly(ethylene imine) was used to achieve a layered structure, and a composite material with alternating PDA and amine domains was obtained after deposition on simple paper strips and UV light-induced polymerization.[218,221] The paper strips were successfully used as sensors to detect friction, and even the cumulative wear upon repeated application of force could be analyzed by using calibration curves, which were obtained by exposure of the strips to different frictional forces (0.2, 1.2, 2.45, and 6.37 N) and subsequent plotting of the red color intensity against the magnitude of the applied forces (**Figure 16c**). This allowed, *e.g.*, to distinguish between the brushing forces of different types of toothbrushes and it was demonstrated that the average forces applied during brushing primarily depend on the hardness of the brush rather than the applied strength (**Figure 16d,e**) and showcases that

the mechanochromic response due to conformational changes of polymers still offers significant potential for novel applications.[218]

6. Conclusions

The use of mechanophores in which covalent bonds are homo- or heterolytically cleaved has, been pivotal for the development of the field of mechanoresponsive and mechanochromic materials, but the controlled scission of non-covalent interactions has more recently emerged as an alternative design strategy. Non-sacrificial mechanoresponsive motifs offer many possibilities for the detection of forces of drastically different magnitude, and the optical signaling of damage can be achieved in a range of different (polymeric) materials. As highlighted in the present review, many different types of non-covalent interactions as well as inter- or intramolecular interactions have in this context been explored to elicit a mechanoresponsive behavior. Akin to covalent mechanophores, the molecules, binding motifs, or polymers that act as the responsive entities generally need to be mechanically stimulated so that an energy barrier is overcome and conformational changes or the dissociation of interacting molecules or binding motifs are affected. Due to the tunable nature of these mechanoresponsive motifs, the activation energy to trigger the desired response is highly variable, and such motifs can be employed in materials with drastically different properties. This includes composite materials as structural components, thermoplastic polymers, soft materials such as gels or elastomers, the detection of strains experienced during the self-assembly processes of polymers, as well as the analysis of comparatively small changes and forces experienced by cell membranes under varying environmental conditions.

The breadth of applications and the relevant mechanical forces that occur in these systems certainly highlights the tunable nature of non-sacrificial mechanoresponsive motifs. In many instances, the dissociation or transformation of these motifs and the corresponding response can be readily reversed, repeated deformation processes can be directly observed, and even monitoring of dynamic processes has been demonstrated. The type of colorimetric response, *i.e.*, changes to the emission or absorption properties, depends on the employed chromogenic units and these directly determine what types of techniques can be used to detect and monitor the effects of applied mechanical forces. Changes in the emission properties remain the most frequent type of response considering the many examples that rely, for example, on the emission from aggregachromic dyes, interactions between chromophores that undergo energy transfer processes, directional non-covalent interactions of luminescent metal-ligand complexes, or conformational changes in fluorescent molecules or polymers. The advances in high (super) resolution microscopy techniques certainly appears to offer many interesting opportunities to exploit such emission changes and monitor mechanically activated events on a molecular level, but direct changes to the absorption color remain to be intriguing targets when aiming to elicit a visually discernible warning signal in materials that are used for structural health monitoring or in tamper-proof packaging applications.

When taking into consideration the many different environments and materials in which mechanochromic responses have by now been successfully achieved through the use of responsive non-covalent interactions, it appears readily conceivable that essentially any type of (polymeric) material can be in principle rendered mechanochromic with the right type of motif. Having said this, the fabrication of highly sensitive mechanoresponsive motifs can require extensive synthetic efforts or the direct modification of the host material, which can impede their actual use. A simplification of the design of these motifs, while at the same maintaining their responsiveness, tunability, and reversibility, therefore constitutes an important challenge that needs to be tackled when envisioning a broad application of non-sacrificial mechanoresponsive motifs as (macro)molecular probes for the detection of mechanical stresses. Moreover, motifs that can be employed in one type of environment frequently do not display an adequate responsive behavior when parameters such as the polymer matrix are changed. Ideally, one may envision, that future mechanoresponsive motifs can be used as additives that are (relatively) simple to prepare, which can be easily blended or integrated into a wide range of different types of materials, while at the same time reliably furnishing a mechanochromic response over a wide range of forces. The different examples that have been discussed in this review certainly provide important insights and highlight the potential of non-sacrificial mechanoresponsive motifs. There also appear to be many unique opportunities at the interface between materials science and biology, and the development of motifs that act as efficient force probes that can be used in both environments could grant access to many interesting applications such as implants with mechanical properties that are adjusted to the biological environment or mechanoresponsive cell growth scaffolds. At the same time, further work needs to be done to explore the limits of the force sensitivity of the different types of mechanoresponsive motifs and to develop strategies that renders such motifs useful for these drastically different environments and applications.

Acknowledgements

Financial support through the National Center of Competence in Research (NCCR) Bio-Inspired Materials, a research instrument of the Swiss National Science Foundation (SNF) as well as funding from the Adolphe Merkle Foundation is gratefully acknowledged. Derek J. Kiebala and Hanna Traeger contributed equally to this work.

Conflict of Interest

The authors declare no conflict of interest.

Received: ((will be filled in by the editorial staff))

Revised: ((will be filled in by the editorial staff))

References

[1] M. K. Beyer, H. Clausen-Schaumann, *Chem. Rev.* **2005**, *105*, 2921.

[2] M. M. Caruso, D. A. Davis, Q. Shen, S. A. Odom, N. R. Sottos, S. R. White, J. S. Moore, *Chem. Rev.* **2009**, *109*, 5755.

[3] Y. C. Simon, S. L. Craig, *Mechanochemistry in Materials*, Royal Society of Chemistry, Cambridge, UK, **2017**.

[4] a) W. D. Callister, D. G. Rethwisch, *Fundamentals of Materials Science and Engineering. An Integrated Approach*, John Wiley & Sons, Inc, Hoboken, NJ, USA, **2019**; b) C. Creton, M. Ciccotti, *Rep. Prog. Phys.* **2016**, *79*, 46601.

[5] N. Deneke, M. L. Rencheck, C. S. Davis, *Soft Matter* **2020**, *16*, 6230.

[6] M. Stratigaki, R. Göstl, *ChemPlusChem* **2020**, *85*, 1095.

[7] J. Li, C. Nagamani, J. S. Moore, *Acc. Chem. Res.* **2015**, *48*, 2181.

[8] J. F. Patrick, M. J. Robb, N. R. Sottos, J. S. Moore, S. R. White, *Nature* **2016**, *540*, 363.

[9] C. Calvino, L. Neumann, C. Weder, S. Schrettl, *J. Polym. Sci. Part A: Polym. Chem.* **2017**, *55*, 640.

[10] C. E. Diesendruck, G. I. Peterson, H. J. Kulik, J. A. Kaitz, B. D. Mar, P. A. May, S. R. White, T. J. Martínez, A. J. Boydston, J. S. Moore, *Nat. Chem.* **2014**, *6*, 623.

[11] P. Shieh, W. Zhang, K. E. L. Husted, S. L. Kristufek, B. Xiong, D. J. Lundberg, J. Lem, D. Veysset, Y. Sun, K. A. Nelson, D. L. Plata, J. A. Johnson, *Nature* **2020**, *583*, 542.

[12] P. Cawley, *Struct. Health Monit.* **2018**, *17*, 1225.

[13] W. H. Binder, *Polymer* **2020**, *202*, 122639.

[14] J. N. Brantley, K. M. Wiggins, C. W. Bielawski, *Polym. Int.* **2013**, *62*, 2.

[15] M. J. Robb, W. Li, R. C. R. Gergely, C. C. Matthews, S. R. White, N. R. Sottos, J. S. Moore, *ACS Cent. Sci.* **2016**, *2*, 598.

[16] D. A. Davis, A. Hamilton, J. Yang, L. D. Cremar, D. van Gough, S. L. Potisek, M. T. Ong, P. V. Braun, T. J. Martínez, S. R. White, J. S. Moore, N. R. Sottos, *Nature* **2009**, *459*, 68.

[17] E. Ducrot, Y. Chen, M. Bulters, R. P. Sijbesma, C. Creton, *Science* **2014**, *344*, 186.

[18] a) R. Göstl, R. P. Sijbesma, *Chem. Sci.* **2016**, *7*, 370; b) X. Hu, M. E. McFadden, R. W. Barber, M. J. Robb, *J. Am. Chem. Soc.* **2018**, *140*, 14073; c) J. Kida, K. Imato, R. Goseki, D. Aoki, M. Morimoto, H. Otsuka, *Nat. Commun.* **2018**, *9*, 3504; d) S. S. M. Konda, J. N. Brantley, B. T. Varghese, K. M. Wiggins, C. W. Bielawski, D. E. Makarov, *J. Am. Chem. Soc.* **2013**, *135*, 12722; e) R. Stevenson, G. de Bo, *J. Am. Chem. Soc.* **2017**, *139*, 16768; f) Z. Wang, S. L. Craig, *Chem. Commun.* **2019**, *55*, 12263.

[19] A. E. M. Beedle, M. Mora, C. T. Davis, A. P. Snijders, G. Stirnemann, S. Garcia-Manyes, *Nat. Commun.* **2018**, *9*, 3155.

[20] Y. Lin, T. B. Kouznetsova, S. L. Craig, *J. Am. Chem. Soc.* **2020**, *142*, 99.

[21] Y. Lin, T. B. Kouznetsova, S. L. Craig, *J. Am. Chem. Soc.* **2020**, *142*, 2105.

[22] T. van de Laar, H. Schuurman, P. van der Scheer, J. van Maarten Doorn, J. van der Gucht, J. Sprakel, *Chem* **2018**, *4*, 269.

[23] A. G. Roessler, P. M. Zimmerman, *J. Phys. Chem. C* **2018**, *122*, 6996.

[24] a) N. Willis-Fox, E. Rognin, T. A. Aljohani, R. Daly, *Chem* **2018**, *4*, 2499; b) S. Akbulatov, R. Boulatov, *ChemPhysChem* **2017**, *18*, 1422.

[25] C. Nagamani, H. Liu, J. S. Moore, *J. Am. Chem. Soc.* **2016**, *138*, 2540.

[26] J. M. Clough, A. Balan, T. L. J. van Daal, R. P. Sijbesma, *Angew. Chem. Int. Ed.* **2016**, *55*, 1445.

[27] a) M. B. Larsen, A. J. Boydston, *J. Am. Chem. Soc.* **2014**, *136*, 1276; b) M. B. Larsen, A. J. Boydston, *J. Am. Chem. Soc.* **2013**, *135*, 8189.

[28] G. I. Peterson, A. J. Boydston, *Macromol. Rapid Commun.* **2014**, *35*, 1611.

[29] Y. Chen, A. J. H. Spiering, S. Karthikeyan, G. W. M. Peters, E. W. Meijer, R. P. Sijbesma, *Nat. Chem.* **2012**, *4*, 559.

[30] a) W. Qiu, P. A. Gurr, G. da Silva, G. G. Qiao, *Polym. Chem.* **2019**, *10*, 1650; b) Z. Cao, *Macromol. Chem. Phys.* **2020**, *221*, 2000190; c) R. Klajn, *Chem. Soc. Rev.* **2014**, *43*, 148; d) M. Bertoldo, S. Nazzi, G. Zampano, F. Ciardelli, *Carbohydr. Polym.* **2011**, *85*, 401.

[31] Z. Shi, J. Wu, Q. Song, R. Göstl, A. Herrmann, *J. Am. Chem. Soc.* **2020**, *142*, 14725.

[32] R. J. Wojtecki, A. Nelson, *J. Polym. Sci. A Polym. Chem.* **2016**, *54*, 457.

[33] A. Campanella, D. Döhler, W. H. Binder, *Macromol. Rapid Commun.* **2018**, *39*, e1700739.

[34] a) K. M. Herbert, S. Schrettl, S. J. Rowan, C. Weder, *Macromolecules* **2017**, *50*, 8845; b) X. Yan, F. Wang, B. Zheng, F. Huang, *Chem. Soc. Rev.* **2012**, *41*, 6042.

[35] L. N. Neumann, C. Weder, S. Schrettl, *Chimia* **2019**, *73*, 277.

[36] Y. Yang, M. W. Urban, *Adv. Mater. Interfaces* **2018**, *5*, 1800384.

[37] a) L. M. de Espinosa, G. L. Fiore, C. Weder, E. Johan Foster, Y. C. Simon, *Prog. Polym. Sci.* **2015**, *49-50*, 60; b) Y. Yang, X. Ding, M. W. Urban, *Prog. Polym. Sci.* **2015**, *49-50*, 34.

[38] a) K. J. Henderson, T. C. Zhou, K. J. Otim, K. R. Shull, *Macromolecules* **2010**, *43*, 6193; b) J. P. Gong, Y. Katsuyama, T. Kurokawa, Y. Osada, *Adv. Mater.* **2003**, *15*, 1155; c) C.-H. Li, C. Wang,

C. Keplinger, J.-L. Zuo, L. Jin, Y. Sun, P. Zheng, Y. Cao, F. Lissel, C. Linder, X.-Z. You, Z. Bao, *Nat. Chem.* **2016**, *8*, 618; d) J.-Y. Sun, X. Zhao, W. R. K. Illeperuma, O. Chaudhuri, K. H. Oh, D. J. Mooney, J. J. Vlassak, Z. Suo, *Nature* **2012**, *489*, 133; e) X. Zhao, *Soft Matter* **2014**, *10*, 672.

[39] a) B. J. B. Folmer, R. P. Sijbesma, R. M. Versteegen, J. A. J. van der Rijt, E. W. Meijer, *Adv. Mater.* **2000**, *12*, 874; b) D. W. R. Balkenende, R. A. Olson, S. Balog, C. Weder, L. Montero de Espinosa, *Macromolecules* **2016**, *49*, 7877; c) M. Burnworth, J. D. Mendez, M. Schroeter, S. J. Rowan, C. Weder, *Macromolecules* **2008**, *41*, 2157; d) L. N. Neumann, I. Gunkel, A. Barron, E. Oveisi, A. Petzold, T. Thurn-Albrecht, S. Schrettl, C. Weder, *Macromolecules* **2020**, *53*, 5068; e) F. Würthner, Z. Chen, F. J. M. Hoeben, P. Osswald, C.-C. You, P. Jonkheijm, J. v. Herrikhuyzen, Schenning, Albertus P. H. J., van der Schoot, Paul P. A. M., E. W. Meijer, E. H. A. Beckers, S. C. J. Meskers, R. A. J. Janssen, *J. Am. Chem. Soc.* **2004**, *126*, 10611; f) M. Burnworth, D. Knapton, S. J. Rowan, C. Weder, *J. Inorg. Organomet. Polym.* **2007**, *17*, 91.

[40] L. Yang, X. Tan, Z. Wang, X. Zhang, *Chem. Rev.* **2015**, *115*, 7196.

[41] F. A. Carey, R. J. Sundberg, *Advanced Organic Chemistry*, Springer Verlag, New York, NY, USA, **2007**.

[42] A. Goujon, A. Colom, K. Straková, V. Mercier, D. Mahecic, S. Manley, N. Sakai, A. Roux, S. Matile, *J. Am. Chem. Soc.* **2019**, *141*, 3380.

[43] S. Chae, J. P. Lee, J.-M. Kim, *Adv. Funct. Mater.* **2016**, *26*, 1769.

[44] C. Calvino, A. Guha, C. Weder, S. Schrettl, *Adv. Mater.* **2018**, *30*, e1704603.

[45] R. Merindol, G. Delechiave, L. Heinen, L. H. Catalani, A. Walther, *Nat. Commun.* **2019**, *10*, 528.

[46] A. D. Das, G. Mannoni, A. E. Früh, D. Orsi, R. Pinalli, E. Dalcanale, *ACS Appl. Polym. Mater.* **2019**, *1*, 2990.

[47] Y. Sagara, M. Karman, E. Verde-Sesto, K. Matsuo, Y. Kim, N. Tamaoki, C. Weder, *J. Am. Chem. Soc.* **2018**, *140*, 1584.

[48] P. Chen, Q. Li, S. Grindy, N. Holten-Andersen, *J. Am. Chem. Soc.* **2015**, *137*, 11590.

[49] H. E. Cingil, I. M. Storm, Y. Yorulmaz, D. W. te Brake, R. de Vries, M. A. Cohen Stuart, J. Sprakel, *J. Am. Chem. Soc.* **2015**, *137*, 9800.

[50] J. Zessin, M. Schnepf, U. Oertel, T. Beryozkina, T. A. F. König, A. Fery, M. Mertig, A. Kiriy, *Adv. Opt. Mater.* **2020**, *8*, 1901410.

[51] J. Kunzelman, B. R. Crenshaw, M. Kinami, C. Weder, *Macromol. Rapid Commun.* **2006**, *27*, 1981.

[52] S. Lörcher, T. Winkler, K. Makyła, C. Ouellet-Plamondon, I. Burgert, N. Bruns, *J. Mater. Chem. A* **2014**, *2*, 6231.

[53] K. Makyła, C. Müller, S. Lörcher, T. Winkler, M. G. Nussbaumer, M. Eder, N. Bruns, *Adv. Mater.* **2013**, *25*, 2701.

[54] A. E. Früh, F. Artoni, R. Brighenti, E. Dalcanale, *Chem. Mater.* **2017**, *29*, 7450.

[55] Z. Qiu, W. Zhao, M. Cao, Y. Wang, J. W. Y. Lam, Z. Zhang, X. Chen, B. Z. Tang, *Adv. Mater.* **2018**, *30*, e1803924.

[56] M. Goktas, K. G. Blank, *Adv. Mater. Interfaces* **2017**, *4*, 1600441.

[57] a) K. C. Neuman, A. Nagy, *Nat. Methods* **2008**, *5*, 491; b) F. M. Fazal, S. M. Block, *Nat. Photonics* **2011**, *5*, 318.

[58] S. Pandey, D. V. D. W. Kankanamalage, X. Zhou, C. Hu, L. Isaacs, J. Jayawickramarajah, H. Mao, *J. Am. Chem. Soc.* **2019**, *141*, 18385.

[59] R. A. Nallicheri, M. F. Rubner, *Macromolecules* **1991**, *24*, 517.

[60] a) M. F. Rubner, *Macromolecules* **1986**, *19*, 2129; b) M. F. Rubner, *Macromolecules* **1986**, *19*, 2114.

[61] V. P.-Y. Ma, K. Salaita, *Elife* **2018**, *7*, e38959.

[62] A. D. Doyle, K. M. Yamada, *Nature* **2010**, *466*, 192.

[63] a) J. Mei, N. L. C. Leung, R. T. K. Kwok, J. W. Y. Lam, B. Z. Tang, *Chem. Rev.* **2015**, *115*, 11718; b) Y. Hong, J. W. Y. Lam, B. Z. Tang, *Chem. Commun.* **2009**, 4332.

[64] J. Luo, Z. Xie, J. W. Lam, L. Cheng, H. Chen, C. Qiu, H. S. Kwok, X. Zhan, Y. Liu, D. Zhu, B. Z. Tang, *Chem. Commun.* **2001**, 1740.

[65] Y. Hong, J. W. Y. Lam, B. Z. Tang, *Chem. Soc. Rev.* **2011**, *40*, 5361.

[66] A. Qin, J. W.Y. Lam, B. Z. Tang, *Prog. Polym. Sci.* **2012**, *37*, 182.

[67] J. Dong, M. Liu, R. Jiang, H. Huang, Q. Wan, Y. Wen, J. Tian, Y. Dai, X. Zhang, Y. Wei, *J. Colloid Interface Sci.* **2018**, *528*, 192.

[68] a) M. M. Islam, Z. Hu, Q. Wang, C. Redshaw, X. Feng, *Mater. Chem. Front.* **2019**, *3*, 762; b) E. R. Jimenez, H. Rodríguez, *J. Mater. Sci.* **2020**, *55*, 1366.

[69] a) W. Z. Yuan, P. Lu, S. Chen, J. W. Y. Lam, Z. Wang, Y. Liu, H. S. Kwok, Y. Ma, B. Z. Tang, *Adv. Mater.* **2010**, *22*, 2159; b) Y. Huang, J. Xing, Q. Gong, L.-C. Chen, G. Liu, C. Yao, Z. Wang, H.-L. Zhang, Z. Chen, Q. Zhang, *Nat. Commun.* **2019**, *10*.

[70] a) Y.-B. Gong, P. Zhang, Y.-r. Gu, J.-Q. Wang, M.-M. Han, C. Chen, X.-J. Zhan, Z.-L. Xie, B. Zou, Q. Peng, Z.-G. Chi, Z. Li, *Adv. Optical Mater.* **2018**, *6*, 1800198; b) Y. Q. Dong, J. W. Y. Lam, B. Z. Tang, *J. Phys. Chem. Lett.* **2015**, *6*, 3429.

[71] a) E. Ubba, Y. Tao, Z. Yang, J. Zhao, L. Wang, Z. Chi, *Chem. Asian J.* **2018**, *13*, 3106; b) Z. Chi, X. Zhang, B. Xu, X. Zhou, C. Ma, Y. Zhang, S. Liu, J. Xu, *Chem. Soc. Rev.* **2012**, *41*, 3878; c) Y. Sagara, T. Kato, *Nat. Chem.* **2009**, *1*, 605.

[72] S. Shree, M. Dowds, A. Kuntze, Y. K. Mishra, A. Staubitz, R. Adelung, *Mater. Horiz.* **2020**, *7*, 598.

[73] a) C. Wang, B. Xu, M. Li, Z. Chi, Y. Xie, Q. Li, Z. Li, *Mater. Horiz.* **2016**, *3*, 220; b) B. Xu, J. He, Y. Mu, Q. Zhu, S. Wu, Y. Wang, Y. Zhang, C. Jin, C. Lo, Z. Chi, A. Lien, S. Liu, J. Xu, *Chem. Sci.* **2015**, *6*, 3236.

[74] X. Lu, W. Li, N. R. Sottos, J. S. Moore, *ACS Appl. Mater. Inter.* **2018**, *10*, 40361.

[75] W. Zhao, Z. He, Q. Peng, J. W. Y. Lam, H. Ma, Z. Qiu, Y. Chen, Z. Zhao, Z. Shuai, Y. Dong, B. Z. Tang, *Nat. Commun.* **2018**, *9*, 3044.

[76] Z. Zhang, M. Cao, Le Zhang, Z. Qiu, W. Zhao, G. Chen, X. Chen, B. Z. Tang, *ACS Appl. Mater. Inter.* **2020**, *12*, 22129.

[77] B. Zhao, C. O'Brien, A. P. K. K. K. Mudiyanselage, N. Li, Y. Bagheri, R. Wu, Y. Sun, M. You, *J. Am. Chem. Soc.* **2017**, *139*, 18182.

[78] P. Yan, A. Xie, M. Wei, L. M. Loew, *J. Org. Chem.* **2008**, *73*, 6587.

[79] Q. Verolet, A. Rosspeintner, S. Soleimanpour, N. Sakai, E. Vauthey, S. Matile, *J. Am. Chem. Soc.* **2015**, *137*, 15644.

[80] a) M. Macchione, N. Chuard, N. Sakai, S. Matile, *ChemPlusChem* **2017**, *82*, 1062; b) S. Soleimanpour, A. Colom, E. Derivery, M. Gonzalez-Gaitan, A. Roux, N. Sakai, S. Matile, *Chem. Commun.* **2016**, *52*, 14450.

[81] H. V. Humeniuk, G. Licari, E. Vauthey, N. Sakai, S. Matile, *Supramol. Chem.* **2020**, *32*, 106.

[82] H. V. Humeniuk, A. Rosspeintner, G. Licari, V. Kilin, L. Bonacina, E. Vauthey, N. Sakai, S. Matile, *Angew. Chem. Int. Ed.* **2018**, *57*, 10559.

[83] L. Michels, V. Gorelova, Y. Harnvanichvech, J. W. Borst, B. Albada, D. Weijers, J. Sprakel, *PNAS* **2020**, *117*, 18110.

[84] S. B. Ebrahimi, D. Samanta, H. F. Cheng, L. I. Nathan, C. A. Mirkin, *J. Am. Chem. Soc.* **2019**, *141*, 13744.

[85] T. Yamakado, K. Otsubo, A. Osuka, S. Saito, *J. Am. Chem. Soc.* **2018**, *140*, 6245.

[86] M. Torelli, F. Terenziani, A. Pedrini, F. Guagnini, I. Domenichelli, C. Massera, E. Dalcanale, *ChemistryOpen* **2020**, *9*, 261.

[87] M. Torelli, I. Domenichelli, A. Pedrini, F. Guagnini, R. Pinalli, F. Terenziani, F. Artoni, R. Brighenti, E. Dalcanale, *Synlett* **2018**, *29*, 2503.

[88] O. Köhler, D. V. Jarikote, O. Seitz, *ChemBioChem* **2005**, *6*, 69.

[89] F. Hövelmann, I. Gaspar, J. Chamiolo, M. Kasper, J. Steffen, A. Ephrussi, O. Seitz, *Chem. Sci.* **2016**, *7*, 128.

[90] F. Hövelmann, I. Gaspar, A. Ephrussi, O. Seitz, *J. Am. Chem. Soc.* **2013**, *135*, 19025.

[91] F. Hövelmann, L. Bethge, O. Seitz, *ChemBioChem* **2012**, *13*, 2072.

[92] F. Lagugné-Labarthet, Y. Q. An, T. Yu, Y. R. Shen, E. Dalcanale, D. K. Shenoy, *Langmuir* **2005**, *21*, 7066.

[93] a) R. Pinalli, J. W. Trzciński, E. Dalcanale, C. Massera, *Acta Crystallogr.* **2019**, *75*, 103; b) M. Giannetto, A. Pedrini, S. Fortunati, D. Brando, S. Milano, C. Massera, R. Tatti, R. Verucchi, M. Careri, E. Dalcanale, R. Pinalli, *Sens. Actuators, B* **2018**, *276*, 340; c) C. Tudisco, A. Motta, T. Barboza, C. Massera, A. E. Giuffrida, R. Pinalli, E. Dalcanale, G. G. Condorelli, *ACS Omega* **2018**, *3*, 9172; d) F. Bertani, N. Riboni, F. Bianchi, G. Brancatelli, E. S. Sterner, R. Pinalli, S. Geremia, T. M. Swager, E. Dalcanale, *Chemistry* **2016**, *22*, 3312.

[94] M. Inoue, K. Ugawa, T. Maruyama, T. Iwasawa, *Eur. J. Org. Chem.* **2018**, *2018*, 5304.

[95] A. Pucci, G. Ruggeri, *J. Mater. Chem.* **2011**, *21*, 8282.

[96] F. Ciardelli, G. Ruggeri, A. Pucci, *Chem. Soc. Rev.* **2013**, *42*, 857.

[97] J. B. Birks, *Nature* **1967**, *214*, 1187.

[98] J. B. Birks, *Rep. Prog. Phys.* **1975**, *38*, 903.

[99] V. Kumar, B. Sk, S. Kundu, A. Patra, *J. Mater. Chem. C* **2018**, *6*, 12086.

[100] a) E. A. Chandross, J. Ferguson, *J. Chem. Phys.* **1967**, *47*, 2557; b) Y. Gao, H. Liu, S. Zhang, Q. Gu, Y. Shen, Y. Ge, B. Yang, *Phys. Chem. Chem. Phys.* **2018**, *20*, 12129.

[101] J. R. Lakowicz, *Principles of Fluorescence Spectroscopy*, Springer, Boston, MA, USA, **2006**.

[102] C. Löwe, C. Weder, *Adv. Mater.* **2002**, *14*, 1625.

[103] B. R. Crenshaw, C. Weder, *Chem. Mater.* **2003**, *15*, 4717.

[104] B. R. Crenshaw, M. Burnworth, D. Khariwala, A. Hiltner, P. T. Mather, R. Simha, C. Weder, *Macromolecules* **2007**, *40*, 2400.

[105] B. R. Crenshaw, C. Weder, *Macromolecules* **2006**, *39*, 9581.

[106] M. Kinami, B. R. Crenshaw, C. Weder, *Chem. Mater.* **2006**, *18*, 946.

[107] J. Lott, C. Weder, *Macromol. Chem. Phys.* **2010**, *211*, 28.

[108] A. Lavrenova, A. Holtz, Y. C. Simon, C. Weder, *Macromol. Mater. Eng.* **2016**, *301*, 549.

[109] F. Donati, A. Pucci, C. Cappelli, B. Mennucci, G. Ruggeri, *J. Phys. Chem. B* **2008**, *112*, 3668.

[110] a) S. Bao, J. Li, K. I. Lee, S. Shao, J. Hao, B. Fei, J. H. Xin, *ACS Appl. Mater. Inter.* **2013**, *5*, 4625; b) A. Battisti, P. Minei, A. Pucci, R. Bizzarri, *Chem. Commun.* **2016**, *53*, 248.

[111] F. Cellini, S. Khapli, S. D. Peterson, M. Porfiri, *Appl. Phys. Lett.* **2014**, *105*, 61907.

[112] F. Cellini, L. Zhou, S. Khapli, S. D. Peterson, M. Porfiri, *Mech. Mater.* **2016**, *93*, 145.

[113] A. Pucci, T. Biver, G. Ruggeri, L. I. Meza, Y. Pang, *Polymer* **2005**, *46*, 11198.

[114] A. Pucci, F. Di Cuia, F. Signori, G. Ruggeri, *J. Mater. Chem.* **2007**, *17*, 783.

[115] A. Pucci, M. Bertoldo, S. Bronco, *Macromol. Rapid Commun.* **2005**, *26*, 1043.

[116] S. Schrettl, D. W. R. Balkenende, C. Calvino, M. Karman, A. Lavrenova, L. N. Neumann, Y. Sagara, E. Verde-Sesto, M. Di Giannantonio, Y. C. Simon, K. M. Fromm, M. Lattuada, C. Weder, *Chimia* **2019**, *73*, 7.

[117] C. Calvino, C. Weder, *Small* **2018**, *14*, e1802489.

[118] C. Calvino, E. Henriet, L. F. Muff, S. Schrettl, C. Weder, *Macromol. Rapid Commun.* **2020**, *41*, e1900654.

[119] C. Calvino, Y. Sagara, V. Buclin, A. P. Haehnel, A. Del Prado, C. Aeby, Y. C. Simon, S. Schrettl, C. Weder, *Macromol. Rapid Commun.* **2019**, *40*, e1800705.

[120] L. J. Fetters, D. J. Lohse, D. Richter, T. A. Witten, A. Zirkel, *Macromolecules* **1994**, *27*, 4639.

[121] J. Chen, A. W. Ziegler, B. Zhao, W. Wan, A. D. Q. Li, *Chem. Commun.* **2017**, *53*, 4993.

[122] F. Cellini, L. Block, J. Li, S. Khapli, S. D. Peterson, M. Porfiri, *Sens. Actuators B Chem.* **2016**, *234*, 510.

[123] A. Zych, A. Verdelli, M. Soliman, R. Pinalli, A. Pedrini, J. Vachon, E. Dalcanale, *Eur. Polym. J.* **2019**, *111*, 69.

[124] Y. Sagara, T. Kato, *Angew. Chem. Int. Ed.* **2008**, *47*, 5175.

[125] Y. Sagara, S. Yamane, T. Mutai, K. Araki, T. Kato, *Adv. Funct. Mater.* **2009**, *19*, 1869.

[126] Y. Sagara, T. Kato, *Angew. Chem. Int. Ed.* **2011**, *50*, 9128.

[127] a) Y. Sagara, T. Kato, *Supramol. Chem.* **2011**, *23*, 310; b) Y. Sagara, C. Weder, N. Tamaoki, *Chem. Mater.* **2017**, *29*, 6145.

[128] Y. Sagara, T. Komatsu, T. Ueno, K. Hanaoka, T. Kato, T. Nagano, *Adv. Funct. Mater.* **2013**, *23*, 5277.

[129] Y. Sagara, T. Komatsu, T. Ueno, K. Hanaoka, T. Kato, T. Nagano, *J. Am. Chem. Soc.* **2014**, *136*, 4273.

[130] L. Wu, C. Huang, B. P. Emery, A. C. Sedgwick, S. D. Bull, X.-P. He, H. Tian, J. Yoon, J. L. Sessler, T. D. James, *Chem. Soc. Rev.* **2020**, *49*, 5110.

[131] E. Haas, M. Wilchek, E. Katchalski-Katzir, I. Z. Steinberg, *PNAS* **1975**, *72*, 1807.

[132] H. Borochov-Neori, M. Montal, *Biochemistry* **1989**, *28*, 1711.

[133] P. Wu, L. Brand, *Anal. Biochem.* **1994**, *218*, 1.

[134] A.-L. Cost, P. Ringer, A. Chrostek-Grashoff, C. Grashoff, *Cell. Mol. Bioeng.* **2015**, *8*, 96.

[135] Y. Chang, Z. Liu, Y. Zhang, K. Galior, J. Yang, K. Salaita, *J. Am. Chem. Soc.* **2016**, *138*, 2901.

[136] Y. Zhao, K. Pal, Y. Tu, X. Wang, *J. Am. Chem. Soc.* **2020**, *142*, 6930.

[137] a) A. Freikamp, A. Mehlich, C. Klingner, C. Grashoff, *J. Struct. Biol.* **2017**, *197*, 37; b) Y. Liu, K. Galior, V. P.-Y. Ma, K. Salaita, *Acc. Chem. Res.* **2017**, *50*, 2915; c) V. P.-Y. Ma, K. Salaita, *Small* **2019**, *15*, e1900961; d) C. Matellan, A. E. del Río Hernández, *ACS Biomater. Sci. Eng.* **2019**, *5*, 3703; e) Y. Murad, I. T. S. Li, *Biophys. J.* **2019**, *116*, 1282; f) M. Prabhune, F. Rehfeldt, C. F. Schmidt, *J. Phys. D: Appl. Phys.* **2017**, *50*, 233001; g) A. Yasunaga, Y. Murad, I. T. S. Li, *Phys. Biol.* **2019**, *17*, 11001.

[138] M. Goktas, C. Luo, R. M. A. Sullan, A. E. Bergues-Pupo, R. Lipowsky, A. Vila Verde, K. G. Blank, *Chem. Sci.* **2018**, *9*, 4610.

[139] M. Taki, T. Yamashita, K. Yatabe, V. Vogel, *Soft Matter* **2019**, *15*, 9388.

[140] J. W. Neubauer, N. Hauck, M. J. Männel, M. Seuss, A. Fery, J. Thiele, *ACS Appl. Mater. Inter.* **2019**, *11*, 26307.

[141] S. Karthikeyan, R. P. Sijbesma, *Macromolecules* **2009**, *42*, 5175.

[142] A.-Y. Jee, M. Lee, *Chem. Phys. Lett.* **2011**, *501*, 287.

[143] Gil Yeroslavsky, Masao Kamimura, Ryo Inoue, Yasuo Kogo, and Kohei Soga, *J. Photopolym. Sci. Technol.* **2018**, *31*.

[144] S. Ogi, K. Sugiyasu, M. Takeuchi, *B. Chem. Soc. Jpn.* **2011**, *84*, 40.

[145] K. P. Goetz, D. Vermeulen, M. E. Payne, C. Kloc, L. E. McNeil, O. D. Jurchescu, *J. Mater. Chem. C* **2014**, *2*, 3065.

[146] R. Gil, M.-G. Guillerez, J.-C. Poulin, E. Schulz, *Langmuir* **2007**, *23*, 542.

[147] R. Gil, J.-C. Fiaud, J.-C. Poulin, E. Schulz, *Chem. Commun.* **2003**, 2234.

[148] A. Lavrenova, J. Farkas, C. Weder, Y. C. Simon, *ACS Appl. Mater. Inter.* **2015**, *7*, 21828.

[149] Y. Sagara, M. Karman, A. Seki, M. Pannipara, N. Tamaoki, C. Weder, *ACS Cent. Sci.* **2019**, *5*, 874.

[150] T. Muramatsu, Y. Sagara, H. Traeger, N. Tamaoki, C. Weder, *ACS Appl. Mater. Inter.* **2019**, *11*, 24571.

[151] K. Imato, R. Yamanaka, H. Nakajima, N. Takeda, *Chem. Commun.* **2020**, *56*, 7937.

[152] J. Longo, C. Yao, C. Rios, N. T. T. Chau, F. Boulmedais, J. Hemmerlé, P. Lavalle, S. M. Schiller, P. Schaaf, L. Jierry, *Chem. Commun.* **2015**, *51*, 232.

[153] J. N. Brantley, C. B. Bailey, J. R. Cannon, K. A. Clark, D. A. Vanden Bout, J. S. Brodbelt, A. T. Keatinge-Clay, C. W. Bielawski, *Angew. Chem. Int. Ed.* **2014**, *53*, 5088.

[154] B. Barstow, N. Ando, C. U. Kim, S. M. Gruner, *PNAS* **2008**, *105*, 13362.

[155] a) J. Saeger, V. P. Hytönen, E. Klotzsch, V. Vogel, *PloS one* **2012**, *7*, e46962; b) Z. Ganim, M. Rief, *PNAS* **2017**, *114*, 11052.

[156] T. Ichimura, H. Fujita, K. Yoshizawa, T. M. Watanabe, *Chem. Commun.* **2012**, *48*, 7871.

[157] T. M. Watanabe, K. Imada, K. Yoshizawa, M. Nishiyama, C. Kato, F. Abe, T. J. Morikawa, M. Kinoshita, H. Fujita, T. Yanagida, *PloS one* **2013**, *8*, e73212.

[158] Y. Wang, H. Wang, M. V. Tran, W. R. Algar, H. Li, *Chem. Commun.* **2020**, *56*, 5556.

[159] a) S. Iwai, T. Q. P. Uyeda, *PNAS* **2008**, *105*, 16882; b) A. S. LaCroix, A. D. Lynch, M. E. Berginski, B. D. Hoffman, *Elife* **2018**, *7*, e33927; c) K. Austen, P. Ringer, A. Mehlich, A. Chrostek-Grashoff, C. Kluger, C. Klingner, B. Sabass, R. Zent, M. Rief, C. Grashoff, *Nat. Cell Biol.* **2015**, *17*, 1597; d) F. Meng, T. M. Suchyna, F. Sachs, *FEBS J.* **2008**, *275*, 3072.

[160] C. F. Chiu, N. Dementev, E. Borguet, *J. Phys. Chem. A* **2011**, *115*, 9579.

[161] a) N. Bruns, D. S. Clark, *Chimia* **2011**, *65*, 245; b) N. Bruns, K. Pustelny, L. M. Bergeron, T. A. Whitehead, D. S. Clark, *Angew. Chem. Int. Ed.* **2009**, *48*, 5666.

[162] M. Di Giannantonio, M. A. Ayer, E. Verde-Sesto, M. Lattuada, C. Weder, K. M. Fromm, *Angew. Chem. Int. Ed.* **2018**, *57*, 11445.

[163] Y. Sha, Y. Zhang, E. Xu, Z. Wang, T. Zhu, S. L. Craig, C. Tang, *ACS Macro Lett.* **2018**, *7*, 1174.

[164] S. J. Choi, J. Kuwabara, Y. Nishimura, T. Arai, T. Kanbara, *Chem. Lett.* **2012**, *41*, 65.

[165] T. Abe, T. Itakura, N. Ikeda, K. Shinozaki, *Dalton Trans.* **2009**, 711.

[166] V. N. Kozhevnikov, B. Donnio, D. W. Bruce, *Angew. Chem. Int. Ed.* **2008**, *47*, 6286.

[167] J. R. Kumpfer, S. D. Taylor, W. B. Connick, S. J. Rowan, *J. Mater. Chem.* **2012**, *22*, 14196.

[168] D. W. R. Balkenende, S. Coulibaly, S. Balog, Y. C. Simon, G. L. Fiore, C. Weder, *J. Am. Chem. Soc.* **2014**, *136*, 10493.

[169] Q. Zhu, K. Vliet, N. Holten-Andersen, A. Miserez, *Adv. Funct. Mater.* **2019**, *29*, 1808191.

[170] P. Michael, W. H. Binder, *Angew. Chem. Int. Ed.* **2015**, *54*, 13918.

[171] M. Biewend, P. Michael, W. H. Binder, *Soft Matter* **2020**, *16*, 1137.

[172] a) S. Naumann, M. R. Buchmeiser, *Catal. Sci. Technol.* **2014**, *4*, 2466; b) M. N. Hopkinson, C. Richter, M. Schedler, F. Glorius, *Nature* **2014**, *510*, 485; c) L.-A. Schaper, S. J. Hock, W. A. Herrmann, F. E. Kühn, *Angew. Chem. Int. Ed.* **2013**, *52*, 270.

[173] B. Hupp, J. Nitsch, T. Schmitt, R. Bertermann, K. Edkins, F. Hirsch, I. Fischer, M. Auth, A. Sperlich, A. Steffen, *Angew. Chem. Int. Ed.* **2018**, *57*, 13671.

[174] G. A. Filonenko, R. R. Fayzullin, J. R. Khusnutdinova, *J. Mater. Chem. C* **2017**, *5*, 1638.

[175] G. A. Filonenko, J. R. Khusnutdinova, *Adv. Mater.* **2017**, *29*, 1700563.

[176] G. A. Filonenko, J. A. M. Lugger, C. Liu, E. P. A. van Heeswijk, M. M. R. M. Hendrix, M. Weber, C. Müller, E. J. M. Hensen, R. P. Sijbesma, E. A. Pidko, *Angew. Chem. Int. Ed.* **2018**, *57*, 16385.

[177] A. Karimata, P. H. Patil, E. Khaskin, S. Lapointe, R. R. Fayzullin, P. Stampoulis, J. R. Khusnutdinova, *Chem. Commun.* **2020**, *56*, 50.

[178] G. A. Filonenko, D. Sun, M. Weber, C. Müller, E. A. Pidko, *J. Am. Chem. Soc.* **2019**, *141*, 9687.

[179] B. Cheng, S. Cui, *Top. Curr. Chem.* **2015**, *369*, 97.

[180] T. Auletta, M. R. de Jong, A. Mulder, F. C. J. M. van Veggel, J. Huskens, D. N. Reinhoudt, S. Zou, S. Zapotoczny, H. Schönherr, G. J. Vancso, L. Kuipers, *J. Am. Chem. Soc.* **2004**, *126*, 1577.

[181] A. Gomez-Casado, H. H. Dam, M. D. Yilmaz, D. Florea, P. Jonkheijm, J. Huskens, *J. Am. Chem. Soc.* **2011**, *133*, 10849.

[182] H. Schönherr, M. W. J. Beulen, J. Bügler, J. Huskens, F. C. J. M. van Veggel, D. N. Reinhoudt, G. J. Vancso, *J. Am. Chem. Soc.* **2000**, *122*, 4963.

[183] S. Zapotoczny, T. Auletta, M. R. de Jong, H. Schönherr, J. Huskens, F. C. J. M. van Veggel, D. N. Reinhoudt, G. J. Vancso, *Langmuir* **2002**, *18*, 6988.

[184] A. Gomez-Casado, P. Jonkheijm, J. Huskens, *Langmuir* **2011**, *27*, 11508.

[185] C. Schmuck, W. Wienand, *Angew. Chem. Int. Ed.* **2001**, *40*, 4363.

[186] a) S. Zou, H. Schönherr, G. J. Vancso, *J. Am. Chem. Soc.* **2005**, *127*, 11230; b) N. Hosono, A. M. Kushner, J. Chung, A. R. A. Palmans, Z. Guan, E. W. Meijer, *J. Am. Chem. Soc.* **2015**, *137*, 6880; c) A. Embrechts, H. Schönherr, G. J. Vancso, *J. Phys. Chem. B* **2008**, *112*, 7359.

[187] a) H. Dietz, T. Bornschlögl, R. Heym, F. König, M. Rief, *New J. Phys.* **2007**, *9*, 424; b) P. López-García, M. Goktas, A. E. Bergues-Pupo, B. Koksch, D. Varón Silva, K. G. Blank, *Phys. Chem. Chem. Phys.* **2019**, *21*, 9145.

[188] A. Fuhrmann, S. Getfert, Q. Fu, P. Reimann, S. Lindsay, R. Ros, *Biophys. J.* **2012**, *102*, 2381.

[189] P. Shrestha, T. Emura, D. Koirala, Y. Cui, K. Hidaka, W. J. Maximuck, M. Endo, H. Sugiyama, H. Mao, *Nucleic Acids Res.* **2016**, *44*, 6574.

[190] S. Lv, D. M. Dudek, Y. Cao, M. M. Balamurali, J. Gosline, H. Li, *Nature* **2010**, *465*, 69.

[191] Z. Guan, J. T. Roland, J. Z. Bai, S. X. Ma, T. M. McIntire, M. Nguyen, *J. Am. Chem. Soc.* **2004**, *126*, 2058.

[192] J. T. Roland, Z. Guan, *J. Am. Chem. Soc.* **2004**, *126*, 14328.

[193] A. M. Kushner, V. Gabuchian, E. G. Johnson, Z. Guan, *J. Am. Chem. Soc.* **2007**, *129*, 14110.

[194] A. M. Kushner, J. D. Vossler, G. A. Williams, Z. Guan, *J. Am. Chem. Soc.* **2009**, *131*, 8766.

[195] J. Chung, A. M. Kushner, A. C. Weisman, Z. Guan, *Nat. Mater.* **2014**, *13*, 1055.

[196] A. Lavrenova, D. W. R. Balkenende, Y. Sagara, S. Schrettl, Y. C. Simon, C. Weder, *J. Am. Chem. Soc.* **2017**, *139*, 4302.

[197] X. Fang, H. Zhang, Y. Chen, Y. Lin, Y. Xu, W. Weng, *Macromolecules* **2013**, *46*, 6566.

[198] Y. Chen, H. Zhang, X. Fang, Y. Lin, Y. Xu, W. Weng, *ACS Macro Lett.* **2014**, *3*, 141.

[199] Y. Sagara, K. Kubo, T. Nakamura, N. Tamaoki, C. Weder, *Chem. Mater.* **2017**, *29*, 1273.

[200] Céline Calvino, *Doctoral Thesis,* University of Fribourg, Switzerland **2018**.

[201] R. J. Young, P. A. Lovell, *Introduction to Polymers*, CRC Press, Boca Raton, FL, USA, **2011**.

[202] a) D. N. Batchelder, *Contemp. Phys.* **1988**, *29*, 3; b) R. E. Martin, F. Diederich, *Angew. Chem. Int. Ed.* **1999**, *38*, 1350; c) H. Meier, U. Stalmach, H. Kolshorn, *Acta Polym.* **1997**, *48*, 379.

[203] a) Y.-J. Cheng, S.-H. Yang, C.-S. Hsu, *Chem. Rev.* **2009**, *109*, 5868; b) C. Dai, B. Liu, *Energy Environ. Sci.* **2020**, *13*, 24; c) D. T. McQuade, A. E. Pullen, T. M. Swager, *Chem. Rev.* **2000**, *100*, 2537.

[204] W. Lee, J. H. Seo, H. Y. Woo, *Polymer* **2013**, *54*, 5104.

[205] H. E. Cingil, E. B. Boz, J. Wang, M. A. C. Stuart, J. Sprakel, *Adv. Funct. Mater.* **2016**, *26*, 1420.

[206] H. E. Cingil, E. B. Boz, G. Biondaro, R. de Vries, M. A. Cohen Stuart, D. J. Kraft, P. van der Schoot, J. Sprakel, *J. Am. Chem. Soc.* **2017**, *139*, 4962.

[207] a) K. Yoshino, K. Nakao, M. Onoda, R. Sugimoto, *J. Phys.: Condens. Matter* **1989**, *1*, 1009; b) K. Yoshino, K. Nakao, M. Onoda, R.-i. Sugimoto, *Solid State Commun.* **1988**, *68*, 513.

[208] Hess, Kanner, Vardeny, *Phys. Rev., B Condens. Matter* **1993**, *47*, 1407.

[209] a) T. Kaniowski, S. Nizioł, J. Sanetra, M. Trznadel, A. Proń, *Synth. Met.* **1998**, *94*, 111; b) E. J. Samuelsen, J. Mårdalen, O. R. Konestabo, M. Hanfland, M. Lorenzen, *Synth. Met.* **1999**, *101*, 98.

[210] T. Shiga, T. Ikawa, A. Okada, *J. Appl. Polym. Sci.* **1998**, *67*, 259.

[211] T. Shiga, A. Okada, H. Takahashi, T. Kurauchi, *J. Mater. Sci. Lett.* **1995**, *14*, 1754.

[212] R. W. Carpick, D. Y. Sasaki, M. S. Marcus, M. A. Eriksson, A. R. Burns, *J. Phys.: Condens. Matter* **2004**, *16*, R679-R697.

[213] J. Liu, J. W. Y. Lam, B. Z. Tang, *Chem. Rev.* **2009**, *109*, 5799.

[214] a) G. Wegner, *Makromol. Chem.* **1972**, *154*, 35; b) G. Wegner, *Z. Naturforsch. B* **1969**, *24*, 824.

[215] a) X. Qian, B. Städler, *Chem. Mater.* **2019**, *31*, 1196; b) J. T. Wen, J. M. Roper, H. Tsutsui, *Ind. Eng. Chem. Res.* **2018**, *57*, 9037; c) D. J. Ahn, J.-M. Kim, *Acc. Chem. Res.* **2008**, *41*, 805.

[216] J. P. Lee, H. Hwang, S. Chae, J.-M. Kim, *Chem. Commun.* **2019**, *55*, 9395.

[217] L. Polacchi, A. Brosseau, R. Métivier, C. Allain, *Chem. Commun.* **2019**, *55*, 14566.

[218] K. Watanabe, H. Imai, Y. Oaki, *J. Mater. Chem. C* **2020**, *8*, 1265.

[219] H. Feng, J. Lu, J. Li, F. Tsow, E. Forzani, N. Tao, *Adv. Mater.* **2013**, *25*, 1729.

[220] D.-H. Park, J. Hong, I. S. Park, C. W. Lee, J.-M. Kim, *Adv. Funct. Mater.* **2014**, *24*, 5186.

[221] H. Terada, H. Imai, Y. Oaki, *Adv. Mater.* **2018**, *30*, e1801121.

Author Biographies

Hanna Traeger is currently a Ph.D. student with Prof. Christoph Weder and Dr. Stephen Schrettl at the Adolphe Merkle Institute Fribourg, Switzerland. She studied chemistry at University of Jena, focusing on polymer synthesis, assembly and characterization and graduated in 2018 under the supervision of Prof. Felix H. Schacher. Her ongoing research focuses on exploiting supramolecular interactions for the development of novel mechanophores.

Derek Kiebala completed his Bachelor's degree in Integrated Science and Chemistry at Northwestern University in Chicago. In the group of Prof. Samuel Stupp, Derek investigated the self-assembly of perylene diimides for hydrogen-producing soft hydrogels. Derek then completed his Master's in Organic Chemistry at KU Leuven in Belgium, where in the group of Prof. Wim Dehaen he researched dipolar cycloaddition chemistry and synthesized novel heterocycles directed at biological targets. Derek is currently completing his Ph.D. with Prof. Christoph Weder and Dr. Stephen Schrettl at the Adolphe Merkle Institute in Fribourg, Switzerland, where he is investigating supramolecular mechanophores and mechanochromic materials.

Christoph Weder is Director of the Adolphe Merkle Institute (AMI) at the University of Fribourg (Switzerland). Chris was educated at ETH Zurich, where, after a postdoctorate at MIT, he also earned a Habilitation. He then assumed a faculty position at Case Western Reserve University before joining the AMI as Professor for Polymer Chemistry and Materials in 2009. His research is focused on bio-inspired, stimuli-responsive polymers and nanomaterials. Chris is an Associate Editor of *ACS Macro Letters*, a member of the Swiss Academy of Technical Sciences, and a Fellow of the American Chemical Society's Division of Polymer Chemistry. He has mentored about hundred PhD students and postdocs.

Stephen Schrettl is a Group Leader at the Adolphe Merkle Institute (AMI) of the University of Fribourg (Switzerland). After studying Chemistry at Free University Berlin with research at ETH Zurich, he received a PhD in Materials Science in 2014 from Ecole Polytechnique Fédérale de Lausanne (EPFL) and carried out postdoctoral research at EPFL and AMI. His research focuses on taking advantage of non-covalent interactions and polymer self-assembly to prepare responsive and functional organic and polymeric materials.

When polymer materials are exposed to wear and tear, the mechanical stresses can deteriorate their properties. Mechanochromic polymers respond to the applied stresses through a signal, which can be used to monitor deformation or assess damage. In this article, an overview is provided of the responses that can be obtained when mechanoresponsive motifs that respond without covalent bond cleavage are used for the preparation of mechanochromic materials.

D. J. Kiebala#, H. Traeger#, Prof. C. Weder*, Dr. S. Schrettl*

From Molecules to Polymers – Harnessing Inter- and Intramolecular Interactions for Mechanochromic Materials

ToC figure: